Redox Biology 48 (2021) 102193

Contents lists available at ScienceDirect

Redox Biology

journal homepage: www.elsevier.com/locate/redox

TRAIL sensitivity of nasopharyngeal cancer cells involves redox dependent upregulation of TMTC2 and its interaction with membrane caspase-3

Deepika Raman [a], Patricia Tay [a], Jayshree L. Hirpara [b], Dan Liu [c], Shazib Pervaiz [a,b,d,e,f,*]

[a] Department of Physiology, Yong Loo Lin School of Medicine, National University of Singapore, Singapore
[b] Cancer Science Institute, National University of Singapore, Singapore
[c] Integrated Science and Engineering Program (ISEP), NUS Graduate School, National University of Singapore, Singapore
[d] NUS Centre for Cancer Research (N2CR), Yong Loo Lin School of Medicine, National University of Singapore, Singapore
[e] National University Cancer Institute, National University Health System, Singapore
[f] Healthy Longevity Translational Research Programme, Yong Loo Lin School of Medicine, National University of Singapore, Singapore

ARTICLE INFO

Keywords:
NPC
TRAIL
Peroxynitrite
Caspase-3
TMTC2

ABSTRACT

Aims: Preferential expression of receptors for TNF-family related apoptosis inducing ligand (TRAIL), DR4 and DR5 makes TRAIL an attractive anti-cancer therapeutic. However, the efficacy of targeting death receptors has not been extensively studied in nasopharyngeal cancer (NPC). Here we investigated TRAIL sensitivity and its underlying mechanism in NPC cell lines, and assessed the potential of TRAIL as a therapeutic option against NPC.
Results: Using two established NPC cell lines, we report the expression of DR4 and DR5, which respond to TRAIL ligation by triggering efficient Type II apoptosis. Mechanistically, early activation of caspase-3 and its membrane recruitment is identified in NPC cell lines, which is associated with, hitherto unreported, interaction with transmembrane and tetratricopeptide repeat containing 2 (TMTC2) in the lipid raft domains. TMTC2 expression is induced upon exposure to TRAIL and involves intracellular increase in peroxynitrite ($ONOO^-$) production. While $ONOO^-$ increase is downstream of caspase-8 activation, it is involved in the upregulation of TMTC2, gene knockdown of which abrogated TRAIL-induced apoptotic execution. Bioinformatics analyses also provide evidence for a strong correlation between *TMTC2* and *DR4* or *caspase-3* as well as a significantly better disease-free survival in patients with high *TMTC2* expression.
Innovation and conclusion: Collectively, redox-dependent execution of NPC cells upon ligation of TRAIL receptors reintroduces the possible therapeutic use of TRAIL in NPC as well as underscores the potential of using TMTC2 as a biomarker of TRAIL sensitivity.

1. Introduction

Nasopharyngeal carcinoma (NPC) presents itself endemically in the south east asian countries and is ethnically concentrated within the southern chinese population with a higher incidence in males over females [1,2]. One of the primary factors in the etiology of NPC is chronic infection with oncogenic gamma herpes Epstein-Barr virus (EBV), which constitutes the overwhelming majority of NPC [1,3]. For patients in the early stages of disease, radiotherapy remains the primary treatment [4–6]. Regrettably, as most patients are diagnosed at a locally advanced stage, the concurrent use of chemotherapy with cisplatin as the primary therapeutic and 5-Fluorouracil as adjuvant chemotherapy forms the established clinical strategy [7–10]. Although the combination of chemotherapy with radiotherapy has enhanced the prognosis of NPC, resistance development is common [11–13]. More importantly, post-radiotherapy mucosal necrosis and debilitating injury to the nasopharynx severely compromise the quality of life. Therefore, alternative strategies to alleviate therapy-associated toxicity and development of resistance are the need of the hour in the management of recalcitrant disease. In this regard, we previously reported the activation of surrogate death receptor signaling (DR4/DR5 upregulation) and enhanced TRAIL (TNF-related apoptosis-inducing ligand) sensitivity in cancer cells rendered resistant to cisplatin. By dint of its death inducing activity and the relatively selective surface expression of DR4/DR5 on a variety of human cancers, TRAIL has been consistently hailed as a tumor suppressor. This is further supported by evidence linking the loss of TRAIL receptor(s) with increased proclivity to tumorigenesis [14–16]. Along similar lines, while strategies to target TRAIL receptors are under

* Corresponding author. Department of Physiology, YLL SoM, National University of Singapore, Singapore.
E-mail addresses: phssp@nus.edu.sg, shazib_pervaiz@nuhs.edu.sg (S. Pervaiz).

https://doi.org/10.1016/j.redox.2021.102193
Received 26 August 2021; Received in revised form 12 November 2021; Accepted 19 November 2021
Available online 20 November 2021

clinical evaluation for the treatment of several cancer types, its role in the potential mitigation of NPC has not yet been evaluated. As such, it is only logical to explore the status of, and sensitivity to, death receptor signaling in NPC cells, which if promising, could serve to reduce the dose of chemo- or/and radio-therapy with the potential to significantly alleviate therapy-induced tissue injury and damage. To that end, a comprehensive insight into TRAIL sensitivity and the downstream mechanism(s) in NPC cells remains unexplored and poorly understood.

The discovery of TRAIL was attributed to its sequence homology with FasL and TNF-α [17]. TRAIL is considered an effective cytokine and a promising therapeutic agent due to its ability to trigger apoptosis through its receptors, TRAIL-R1 (DR4) and TRAIL-R2 (DR5) [18]. TRAIL induces oligomerization of the membrane receptors, thus facilitating the recruitment of the adaptor protein FADD (Fas Associated Death Domain) and pro-caspase-8. This complex is termed as the Death Inducing Signaling Complex (DISC) and serves as the platform for the dimerization and auto-activation (cleavage) of pro-caspase-8 to active caspase-8. Notably, depending upon the cell type, robust activation of caspase-8 results in the direct activation of caspase-3 (Type I cells) to execute extrinsic apoptosis, whereas cells that fail to induce strong caspase-8 activation are dependent on mitochondrial amplification factors, such as cytochrome C and Smac/Diablo, for apoptosome-dependent caspase-9 activation to trigger intrinsic apoptosis [18]. Also, specific intracellular redox milieux seem to impact death receptor signaling differently, as demonstrated by the ability of superoxide ($O_2^{\cdot-}$) to block and hydrogen peroxide (H_2O_2) to amplify death-receptor-induced apoptosis (including TRAIL-mediated execution) of cancer cells [19–22]. The intricate crosstalk between TRAIL signaling and cellular redox metabolism is further corroborated by the increase in and/or involvement of reactive nitrogen species, namely $ONOO^-$, downstream of DR4/DR5 ligation [21].

Here we set out to investigate the status of TRAIL responsiveness of NPC cell lines in an attempt to evaluate the therapeutic efficacy of death receptor targeting as a potential treatment modality. Results show significant expression of TRAIL receptors in NPC cell lines and in primary cells derived from NPC patients. More importantly, evidence is presented for the existence of a novel signaling circuit upon exposure of NPC cells to TRAIL, which in addition to the classical caspase-8 activation underscores the somewhat less well-described membrane localization of caspase-3 as well as $ONOO^-$-dependent induction of Transmembrane and tetratricopeptide repeat containing 2 (TMTC2) protein. TMTC2 has been described as an integral membrane protein involved in multi-protein complexes, particularly with ER resident proteins, and associated with the regulation of intracellular Ca^{2+} oscillations [23]. We present evidence for a novel mechanism through which TRAIL executes NPC cells and uncovered a novel biomarker TMTC2,

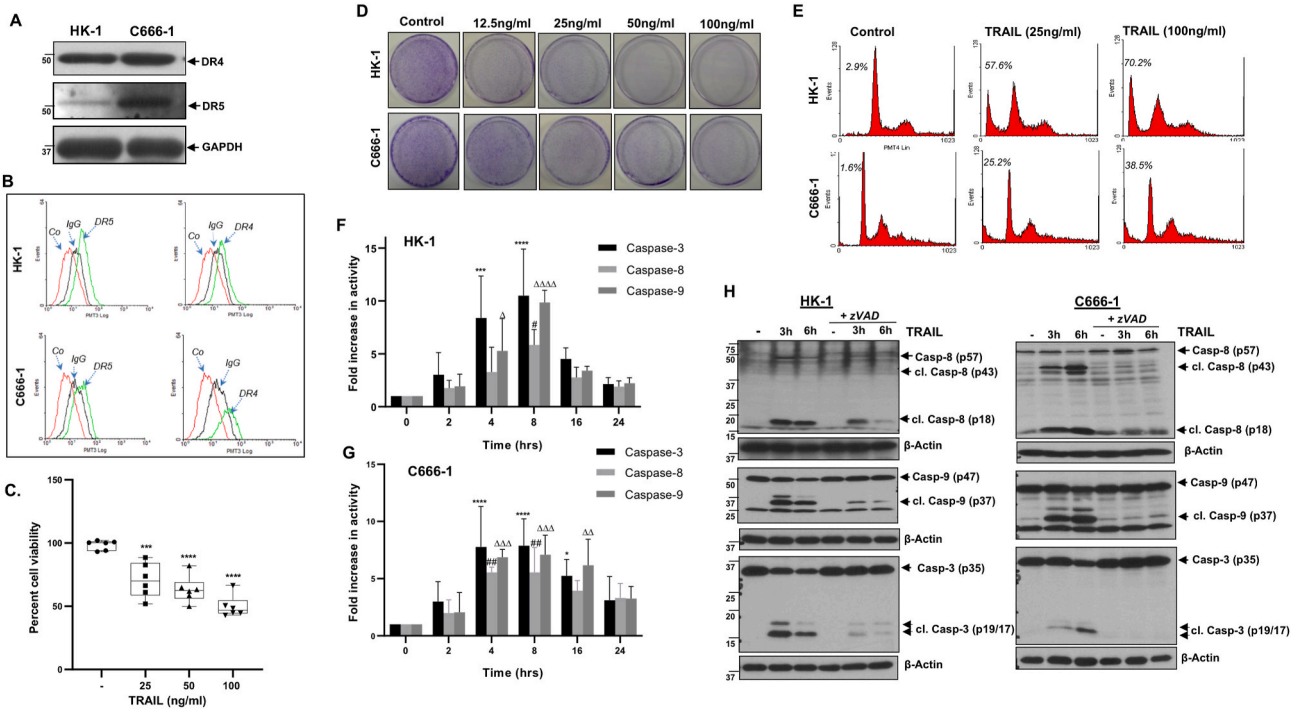

Fig. 1. NPC cell lines express DR4 and DR5 and are sensitive to TRAIL-induced apoptosis (A) Basal protein expression of TRAIL receptors, DR4 and DR5, in HK-1 and C666-1 cells was discerned by Western blot analysis and (B) surface expression was determined by flow cytometry using PE-conjugated mouse monoclonal anti-human DR5 or DR4 as described in Materials and Methods. The same 'no antibody' and 'IgG antibody' stained samples were used as control for plotting individual DR4/DR5 shifts in the respective cell lines. (C) HK-1 cells (0.1×10^6/well plated 48 h before treatment) were treated with increasing concentrations of TRAIL (25–100 ng/ml) for 24 h and cell viability was determined by crystal violet staining as described in Materials nad Methods. One-way ANOVA analysis was used for statistical significance and all comparisons were normalized to untreated control (*** = $p < 0.001$, **** = $p < 0.0001$). (D) HK-1 cells (0.1×10^6/well) or C666-1 cells (0.2×10^6/well) were plated 48 h before exposure to increasing concentrations of TRAIL (0–100 ng/ml) for 8 h and 16 h, respectively, and colony formation was assessed as described in Materials and Methods. (E) HK-1 and C666-1 cells (1×10^6/ml) were treated with 25 ng/ml or 100 ng/ml of TRAIL for 24 h and loaded with PI for cell cycle anlysis. Apoptotic cells are indicated by the % sub-G1 populations. (F) HK-1 cells (0.4×10^6/well) or (G) C666-1 cells (0.8×10^6/well) were seeded in 6-well plates 48 h prior to exposure with 25 ng/ml (HK-1) or 100 ng/ml (C666-1) for 2, 4, 8, 16 and 24 h. Lysates were then used to determine caspase activities using AFC-conjugated substrates as described in Materials and Methods. Two-way ANOVA was employed for statistical analysis and all comparisons were normalized to untreated control (0 h) (* = $p < 0.05$, *** = $p < 0.001$, **** = $p < 0.0001$ *for caspase-3 activity;* # = $p < 0.05$, ## = $p < 0.01$ *for caspase-8 activity;* Δ = $p < 0.05$, ΔΔ = $p < 0.01$, ΔΔΔ = $p < 0.001$, ΔΔΔΔ = $p < 0.0001$ *for caspase 9 activity*). (H) HK-1 cells or C666-1 cells were incubated for 3 h or 6 h with TRAIL (25 ng/ml for HK-1 or 100 ng/ml for C666-1) with or without 1 h pre-incubation with 50 μM Z-VAD-fmk and lysates were subjected to SDS-PAGE Western blot analysis using specific antibodies against caspase-8, -9, or -3 as described in Materials and Methods. . (For interpretation of the references to colour in this figure legend, the reader is referred to the Web version of this article.)

which could potentially be employed to predict sensitivity of cancer cells to TRAIL-mediated execution.

2. Results

2.1. NPC cells express DR4 and DR5 and exhibit sensitivity to TRAIL

In this study, we employed two NPC cell lines, HK-1 and C666-1, to gain mechanistic insight into the role of TRAIL as a potential therapeutic. To that end, we first looked at expression of the functional TRAIL receptors, DR4 and DR5, by western blotting as well as flow cytometry. Both cell lines exhibited basal expression of the death receptors in the whole cell lysate and more importantly on the cell surface (Fig. 1A&B). Exposure of HK-1 cells to incremental doses of TRAIL (0–100 ng/ml) for 24 h showed a dose-dependent decline in cell viability, measured by the crystal violet assay (Fig. 1C). We also performed a colony forming assay, wherein both HK-1 and C666-1 cells were treated with 0–100 ng/ml of TRAIL for 8 h and 16 h, respectively. TRAIL exposure led to a decrease in the colony forming ability in both cell lines, albeit the effect was more pronounced in HK-1 cells than in C666-1 cells (Fig. 1D). Furthermore, to evaluate classical apoptotic signaling, TRAIL-treated cells (25 ng/ml and 100 ng/ml) were evaluated for sub-diploid population by propidium iodide staining and cell cycle analysis as well as caspase-3, -8 and -9 activities and processing. Results show a significant increase in the sub-diploid population, indicative of apoptosis-associated DNA fragmentation, in both cell lines (Fig. 1E); HK-1 cells significantly more sensitive (sub-diploid: 57% at 25 ng/ml and 70% at 100 ng/ml) than C666-1 cells (sub-diploid; 25% at 25 ng/ml and 38% at 100 ng/ml). Based on the differential sensitivities, for all subsequent experiments TRAIL concentration of 25 ng/ml was employed for HK-1 cells while 100 ng/ml was used for C666-1 cells, unless otherwise mentioned. Providing further support to the activation of classical death receptor signaling, an early increase (2 h post TRAIL ligation) in enzymatic activities of caspase-8, -9 and -3, peaking at 8 h post-treatment, were observed in both cell lines (Fig. 1F&G). Caspase activity assessment was further confirmed by the processing of individual caspases upon 3 h or 6 h exposure to TRAIL in the presence or absence of the pan-caspase inhibitor zVAD-fmk. Death receptor ligation resulted in the processing of caspase-8, -9 and -3 into their active forms as detected by Western blot analyses (Fig. 1H). In addition, *a priori* treatment with zVAD-fmk significantly blocked processing of the three caspases, with the strongest effect observed on the executioner caspase-3. Providing further support to the activation of caspase-dependent apoptosis, zVAD-fmk blocked the effect of TRAIL on cell viability (Supplementary Figure S1A&B). Taken together, these data potentiate the ability of TRAIL to induce caspase-dependent apoptotis in NPC cells lines, HK-1 and C666-1.

Next, to assess the functional contribution of DR4 or DR5 to TRAIL sensitization in the two cell lines, we made use of blocking antibodies (anti-DR4 or anti-DR5) and siRNA-mediated gene silencing of *DR4* or *DR5*. While blocking antibodies to DR4 and DR5 (6 h prior to the addition of TRAIL) inhibited the effect of TRAIL on both cell lines (Fig. 2A&B), the effect of *siDR4* was significantly stronger than *siDR5* (Fig. 2C&D). These data suggest the preferential contribution of DR4 to TRAIL-mediated execution of NPC cells, which is in agreement with other studies indicating a dominant functional involvement of one or the other death receptor [24–29].

Despite the fact that caspase-8 serves as the initiator caspase in Type I death receptor signaling, we also observed an early and significant increase in caspase-3 activity, which also suggests the involvement of mitochondrial pathway (Type II), supported by the increase in casapase-9 activity (Fig. 1F&G). Indeed, further evidence implicating mitochondrial amplification pathway is provided by the detection of truncated Bid (t-Bid), a substrate of caspase-8, upon 6 h incubation with TRAIL in HK-1 and C666-1 cells (Fig. 3A). Furthermore, a drop in mitochondrial transmembrane potential ($\Delta\Psi_m$) together with cytosolic translocation of cytochrome C (cyt.C) were observed upon treatment with TRAIL (Fig. 3B&C), indicating mitochondrial outer membrane permeabilization (MOMP). Corroborating the latter, transient overexpression of

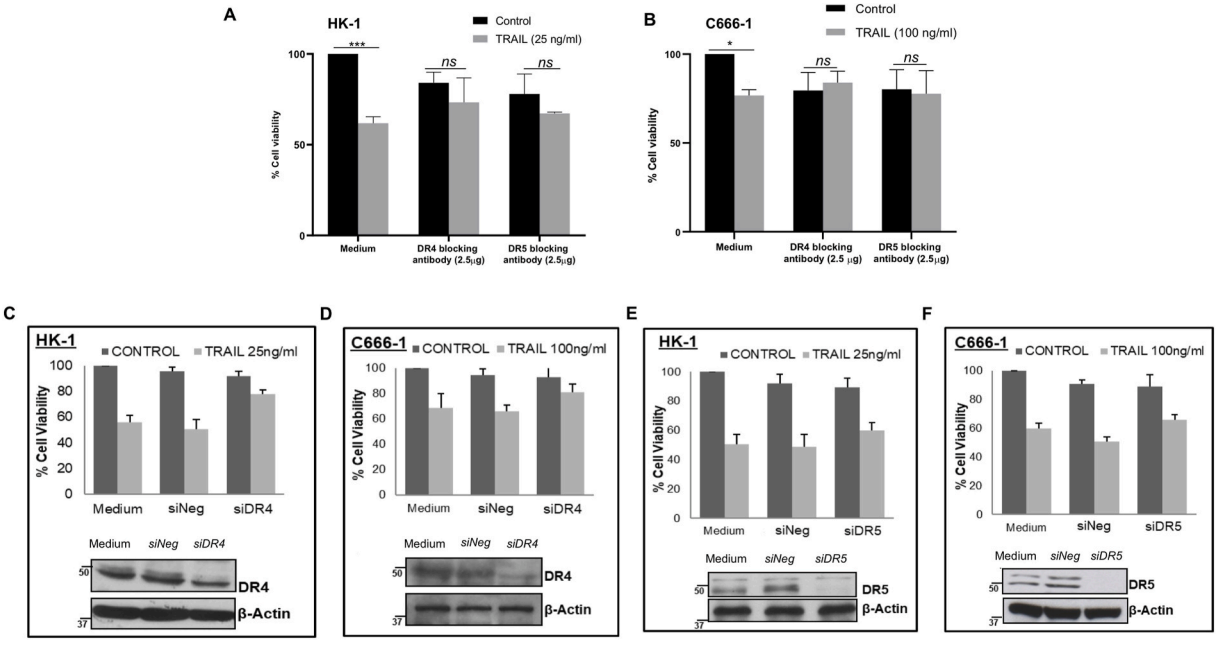

Fig. 2. Blocking DR4 and DR5 allevaites TRAIL-induced apoptosis in NPC cells (A and B) HK-1 cells or C666-1 cells were preincubated for 1 h with anti-DR4 or anti-DR5 blocking antibodies (2.5 μg) followed by exposure to TRAIL (25 ng/ml for HK-1 or 100 ng/ml for C666-1) for 24 h and cell viability was determined by crystal violet staining. Two-way ANOVA was employed for statistical analysis and all comparisons were normalized to control samples treated with culture medium (*$* = p < 0.05$, *$*** = p < 0.001$*). (C and D) Gene expression of *DR4* was knocked down by 48 h transfection with *siDR4* (100 nM) in HK-1 and C666-1 cells followed by 24 h treatment with TRAIL (as above) and cell viability was determined by crystal violet staining. (E and F) DR5 knockdown was attained by *siDR5* (50 nM) transfection over 24 h followed by exposure to TRAIL for 24 h and viability was determined by crystal violet staining. Protein levels of DR4and DR5 following gene knockdown was verified by Western blot analysis using monoclonal anti-DR4 or anti-DR5.

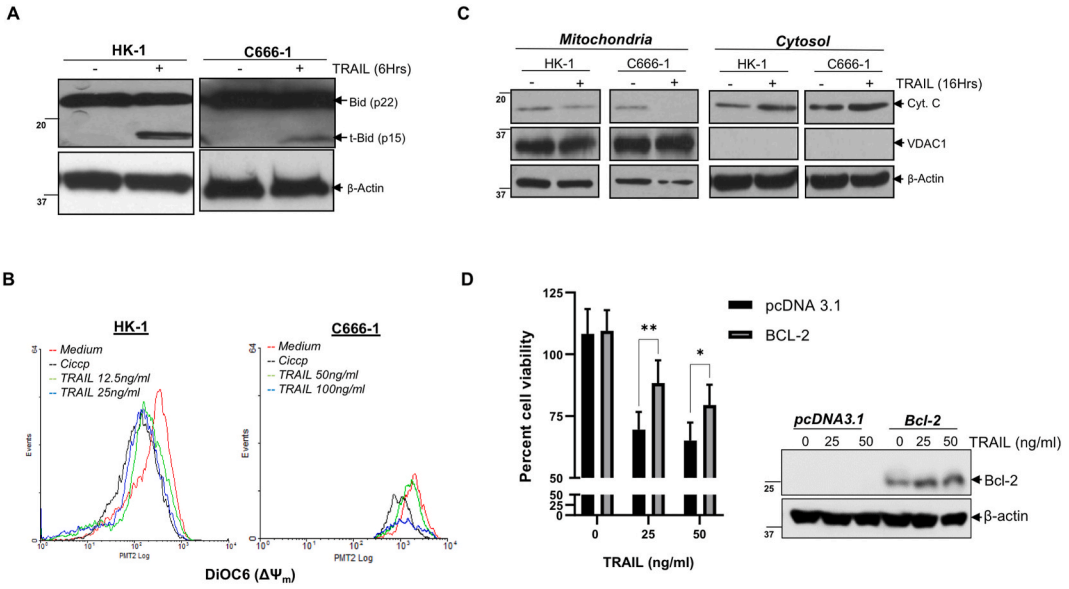

Fig. 3. TRAIL triggers intrinsic apoptosis in NPC cells (A) HK-1 and C666-1 cells were incubated for 6 h withTRAIL (25 ng/ml or 100 ng/ml, respectively) and cell lysates were subjected to SDS-PAGE and Western blot analysis using anti-Bid that picks up pro- and truncated (t-Bid) forms of Bid. (B) HK-1 and C666-1 cells were treated with TRAIL (12.5 ng/ml and 25 ng/ml for HK-1; 50 ng/ml and 100 ng/ml for C666-1) for 2 h followed by loading with DiOC6 (1 μM for 30 min). CiCCP (1 μM) was used as a positive control. At least 10,000 events were analyzed by flow cytometry using WinMDI. Data shown are representative of at least 3 independent experiments. (C) HK-1 and C666-1 cells were treated for 16 h with 25 ng/ml or 100 ng/ml of TRAIL, respectively. Cytoslic and mitochondrial fractions were prepared as described in Materials and Methods and the presence of cytochrome *c* was detected by Western blot using anti-cyt. C. (D) HK-1 cells were transiently transfected with *pcDNA3.1* or *pcDNA3.1-Bcl-2* (2 μg) for 24 h followed by 24 h treatment with TRAIL (25 ng/ml or 50 ng/ml). Data shown are mean ± S.D. of at least three independent experiments. Cell viability was determined by the MTT cell viability assay. Bcl-2 protein expression was verified in the whole cell lysates from vector alone opr Bcl-2 transfected cells by Western blot anlysis using anti-Bcl-2.

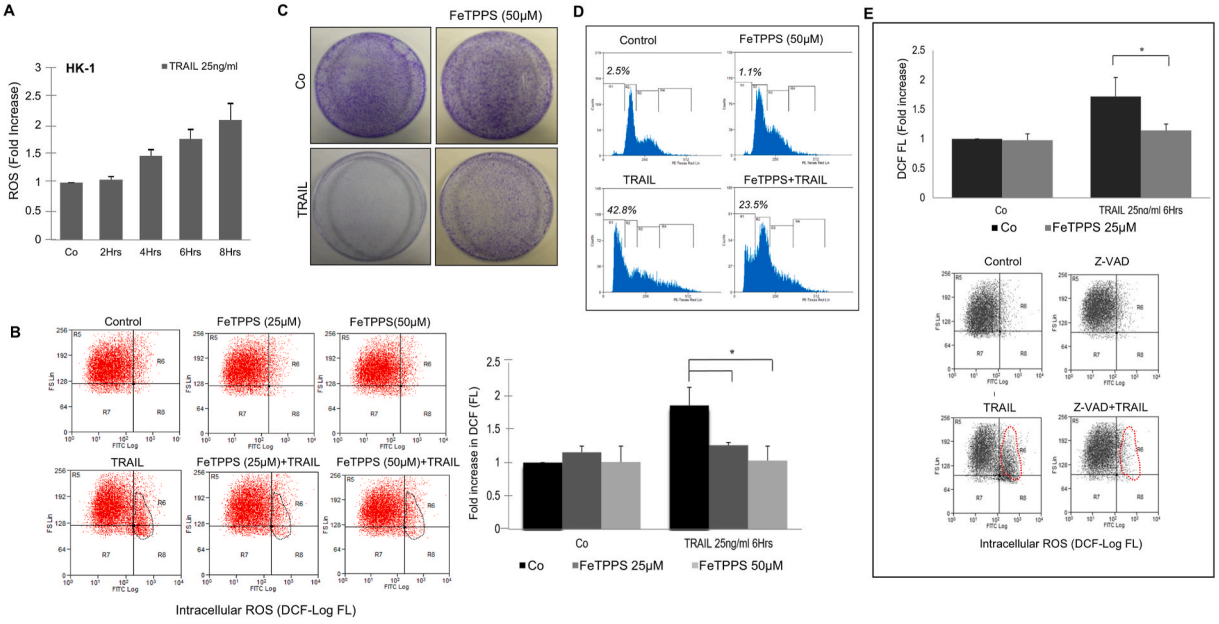

Fig. 4. TRAIL induced apoptotic signaling is a function of intracellular ONOO$^-$ (A) HK-1 cells were treated with 25 ng/ml of TRAIL for 2 h, 4 h, 6 h and 8 h followed by staining with the ROS sensitive probe H2DCFDA (10 μM for 20 min). Flow cytomtery was used to detect an increase in fluorescence. Data from at least three independent experiments were analyzed and presented as Mean ± S.D. of fold changes over the untreated control cells (B) HK-1 cells were pre-incubated with FeTPPS (25 μM and 50 μM) for 1 h followed by 6 h treatment with TRAIL (25 ng/ml). Cells were harvested for flow cytometric analysis using H2DCFDA (10 μM for 20 min). Density plots of forward scatter (Y-axis) against DCFDA fluorescence (x-axis) are shown. Data shown are representative of at least 3 independent experiments. Bar graphs indicating x-fold increase in fluorescence are plotted from three independent experiments and expressed as Mean of fold increase ± S.D. Student's t-test was employed for statistical analysis (* $=p < 0.05$). (C) HK-1 cells were treated with TRAIL as above with or without *a priori* exposure to FeTPPS (50 μM) and colony forming ability was assessed as described in Materials and Methods. (D) HK-1 cells were treated with TRAIL (25 ng/ml) for 24 h with or without 1 h pre-incubation with 50 μM FeTPPS and sub-G1 content (%) was assessed by PI staining and flow cytomtery as described in Materials and Methods. (E) HK-1 cells were treated with 25 ng/ml TRAIL for 6 h with or without 25 μM Z-VAD-fmk and intracellular ROS was detected by loading with 10 μM H2DCFDA and analyzed by flow cytometry as described in Materials and Methods. Student's t-test was used for statistical analysis ($* = p < 0.05$) of data obtained from the independent experiments. Dot plot of DCF-positive (X-axis) cells from a representative flow analysis is shown.

apoptosis inhibitory protein Bcl-2 conferred protection against TRAIL-mediated apoptosis (Fig. 3D). These results support the engagement of intrinsic apoptosis (mitochondrial mediated) in NPC cell lines upon triggering death receptor signaling.

2.2. TRAIL induced apoptosis in NPC cells is mediated by intracellular peroxynitrite generation

Our earlier work provide evidence that changes in cellular redox milieu impact death receptor signaling with both an inhibitory or a sensitizing activity, depending upon the type and concentration of ROS [22,30,31] Of note, we report here a steady increase in intracellular ROS, measured by the increase in DCFDA fluorescence, upon exposure of HK-1 cells to TRAIL for 2 h to 8 h (Fig. 4A). Furthermore, pre-treatment of cells for 1 h with FeTPPS ($ONOO^-$ decomposition catalyst), but not the hydrogen peroxide (H_2O_2) scavenger catalase (4000 Units/ml; data not shown), followed by 6 h incubation with TRAIL (25 ng/ml) significantly blocked the increase in DCFDA fluorescence, thereby supporting the increase in intracellular $ONOO^-$ upon TRAIL treatment (Fig. 4B). Importantly, *a priori* incubation with FeTPPS (1 h) significantly blunted the effect of TRAIL (25 ng/ml for 8 h) on HK-1 cells' colony forming ability (Fig. 4C) and sub-diploid fraction (23.5% vs 42.8%) by PI staining (Fig. 4D). Notably, TRAIL-induced increase in intracellular $ONOO^-$ was rescued in the presence of zVAD-fmk in HK-1 cells, thus placing caspase activation upstream of ROS production (Fig. 4E). Notably, in line with our earlier findings, scavenging $ONOO^-$ also partially blocked TRAIL-induced caspase processing, in particular caspase-8 (Supplementary Figure S1C), thus suggesting a positive feedback loop whereby initial caspase activation induces ROS production which in turn further amplifies caspase activity.

2.3. Novel association between Caspase-3 and transmembrane protein TMTC2 in NPC cells

Intrigued by the relatively early and robust activation of caspase-3 upon TRAIL ligation, we set out to investigate the sub-cellular localization of caspase-3. In this regard, there is evidence, albeit scant, to link early activation of effector caspases to their presence in the lipid raft domains of the plasma membrane [32,33]. To test that, whole cell lysates from HK-1 and C666-1 cells in Triton-X containing buffer were subjected to ultracentrifugation for 21 h in a sucrose gradient and 9 fractions were obtained. A typical feature of lipid rafts is their resistance to extraction by the non-ionic detergent Triton-X in sucrose-containing density gradient at 4 °C. The authenticity of lipid rafts in fractions 4–8 was confirmed by the presence of flotillin, a bonafide lipid raft protein. Interestingly, caspase-3 was detected in fractions 5–9 (Fig. 5A), thus indicating its presence in the lipid raft domains. Furthermore, confocal microscopy was employed to visualize the surface expression of caspase-3 in HK-1 and C666-1 cells using caveolin-1 as a lipid raft marker. Indeed, colocalization of caspase-3 and caveolin-1 was observed in both cell lines (Fig. 5B).

Conventionally, caspase-3 is not described as a membrane-associated protein, which was confirmed by the lack of a membrane localizing signal using the iPSORT prediction software (Supplementary

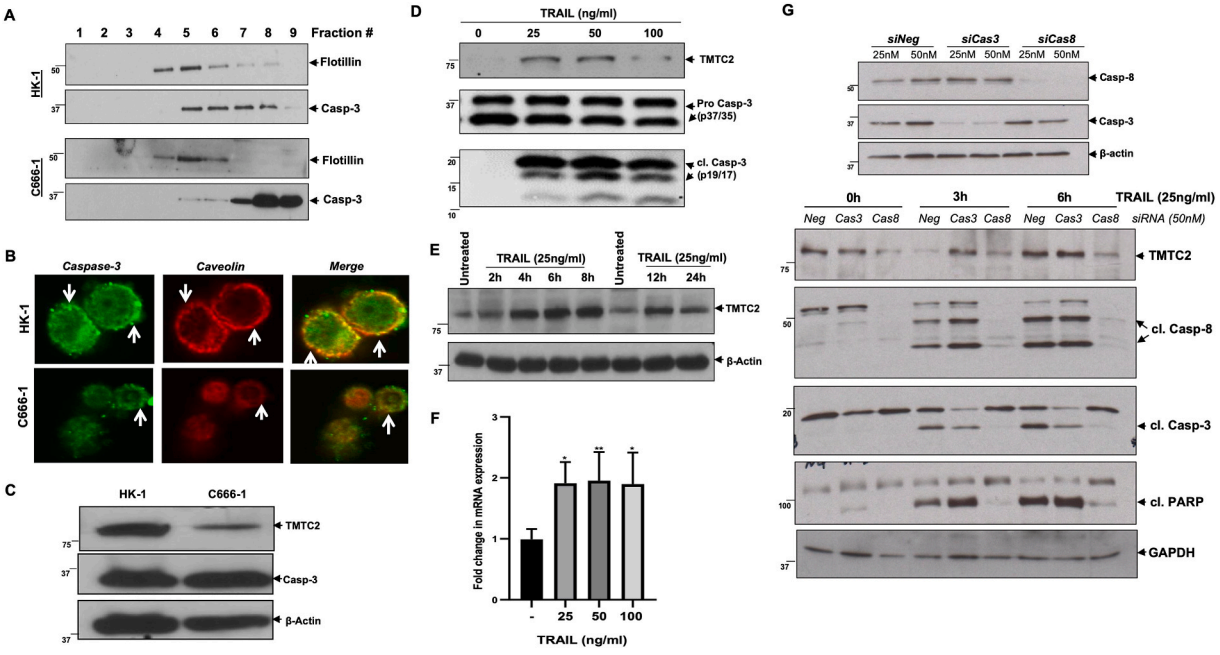

Fig. 5. Membrane lipid raft localization of caspase-3 coincides with TMTC2 which is induced by TRAIL (A) Caspase-3 is detected in the lipid raft fractions of NPC cells. HK-1 and C666-1 cells were harvested for sucrose-gradient ultracentrifugation as described in Materials and Methods . Subsequently, 9 equal fractions were obtained and each fraction was used to analyze for caspase-3 and lipid raft marker flotillin using SDS-PAGE and Western blotting. (B) HK-1 and C666-1 cells were plated on glass-bottom chambers and surface expression of caspase-3 associated with lipid-raft marker caveolin was detected by confocal microscopy as described in Materials and Methods. Arrows indicate co-localization. (C) TMTC2 is expressed in NPC cell lines. Whole cell lysates from HK-1 or C666-1 cells were subjected to SDS-PAGE and probed using anti-TMTC2 or anti-caspase-3 by Western blotting. (D) TRAIL induces TMTC2 and caspase-3 processing. HK-1 cells were treated with increasing concentrations of TRAIL (25–100 ng/ml) for 6 h and whole cell lysates were assessed for TMTC2, pro-caspase-3 and cleaved caspase-3 levels by Western blotting. (E) HK-1 cells were treated with 25 ng/ml of TRAIL for 2 h, 4 h, 6 h, 8 h, 16 h and 24 h and whole cell lysates were probed for TMTC2 by SDS-PAGE and Western blotting using anti-TMTC2 as described in Materials and Methods (F) TRAIL induces *TMTC2 mRNA*. HK-1 cells were treated with TRAIL (25–100 ng/ml) for 6 h and QPCR analyses of *TMTC2* expression was performed as described in Materials and Methods. One-way ANOVA was employed for statistical analysis and all comparisons were normalized to untreated control ($* = p < 0.05$, $** = p < 0.01$). (G) Knock-down of caspase-8, but not caspase-3 prevents TRAIL-mediated induction of TMTC2. *siCasp8 or siCasp3* were used at 25 nM or 50 nM for 48 h for specific gene silencing in HK-1 cells and verified by Western blotting. Following 48 h of gene knockdown cells were treated with TRAIL (25 ng/ml) for 6 h and the expression levels of TMTC2, active caspase-8 (cl-casp-8), active-caspase-3 (cl-casp-3) andPARP cleavage (cl-PARP) were assessed by Western blotting.

Figure S2A). Therefore, to identify potential binding partners that might recruit caspase-3 to the membrane, we immunoprecipitated caspase-3 and resolved the interacting partners by SDS-PAGE. The samples were then subjected to MALDI TOF-TOF analysis (service provided by Protein and Proteomics Centre at DBS, NUS). A potential candidate, transmembrane and tetratricopeptide repeat containing 2 protein (TMTC2), a multi-pass membrane protein containing 10 tetratricopeptide repeats (TPR) was identified. As very little is known about the biological activity of this multi-pass membrane protein in cancer cell fate signaling, we first analyzed TMTC2 expression and the effect of TRAIL ligation on its cellular levels. Results show that TMTC2 is constitutively expressed across a panel of human cancer cell lines (Suplementary Figure S2B). Furthermore, in the NPC model cell lines used in this study, TMTC2 protein expression was significantly higher in HK-1 cells than C666-1 cells (Fig. 5C), which incidentally also exhibited higher sensitivity to TRAIL (than C666-1); also TMTC2 co-localized with caspase-3 and flotillin in the membrane fraction of HK-1 cells (Figure S2C). Notably, a dose and time-dependent upregulation of TMTC2 was observed upon incubation with TRAIL, starting at 4 h following the ligation of the death receptors and sustained for up to 24 h post-treatment (Fig. 5D&E). TRAIL-induced upregulation of TMTC2 appears to be at the level of gene transcription as evidenced by almost a two-fold increase in *TMTC2 mRNA* (Fig. 5F). Furthermore, to ascertain whether TRAIL-induced induction of TMTC2 was a function of caspase activation, siRNA-mediated knockdown of *caspase-8* or *caspase-3* was performed (Fig. 5G). While cells transfected with *siCasp3* did not affect TRAIL-induced upregulation of TMTC2 (TRAIL:25 ng/ml for 3–6 h), *siCasp8* inhibited the effect of TRAIL on TMTC2 expression and apoptotic execution (cl. Caspase-3 and cl. PARP) (Fig. 5G). Collectively, these data provide evidence that TMTC2 is induced upon TRAIL ligation, downstream of the initiator caspase, caspase-8, but upstream of the executioner caspase-3.

2.4. *TMTC2 co-precipitates with caspase-3 and TRAIL-induced upregulation is ONOO⁻-dependent*

To ascertain if TMTC2 acted as a chaperone to transport caspase-3 from the cytosol to the membrane fraction, we transiently knocked-down *TMTC2* by siRNA. Firstly, as shown in the preceding section, TMTC2 co-localized with caspase-3 and flotillin in the membrane fraction of HK-1 cells, and secondly cells transiently transfected with *siTMTC2* showed a significant decrease in membrane recruitment of caspase-3 (Fig. 6A). Of note, TMTC2 co-immunoprecipitated with caspase-3, which further increased upon TRAIL treatment, and the interaction between the two proteins was localized to the membrane lipid raft fraction (Fig. 6B&C). Furthermore, as TMTC2 and related proteins (TMTC 1, 3, and 4) share structural domains that are suggestive of endoplasmic reticulum (ER) resident proteins, we also queried whether ER stress response could also be a stimulus for its upregulation. Interestingly, while exposure of HK-1 cells to thapsigragin or tunicamycin triggered ER stress as evidenced by upregulation of GRP78, there was no effect on TMTC2 expression (Fig. 6D).

Having shown that TRAIL treatment of NPC cells resulted in upregulation of TMTC2 and $ONOO^-$-mediated apoptotic execution of cells, we next investigated the sequence of these two events upon ligation of the death receptors. First, results show that pre-treatment with $ONOO^-$ scavenger, FeTPPS, inhibited the increase in TMTC2 expression induced by TRAIL (Fig. 6E). Second, exogenous addition of $ONOO^-$ significantly upregulated TMTC2 in a dose and time dependent manner (Fig. 6F&G). In addition, the significant increase in *TMTC2 mRNA* induced by TRAIL was not observed in the presence of FeTPPS (Supplementary Figure S3A) while low concentrations (50 μM) of exogenous $ONOO^-$ induced a significant increase in *TMTC2* (Supplementary Figure S3B). Notably, TMTC2 levels remained unaffected by increases in either $O_2^{\cdot-}$ induced upon pharmacological inhibition of SOD1 (DDC) or exogenous addition of H_2O_2 (Supplementary Figure S3C). These data provide evidence that TRAIL-induced upregulation of TMTC2 is redox dependent and

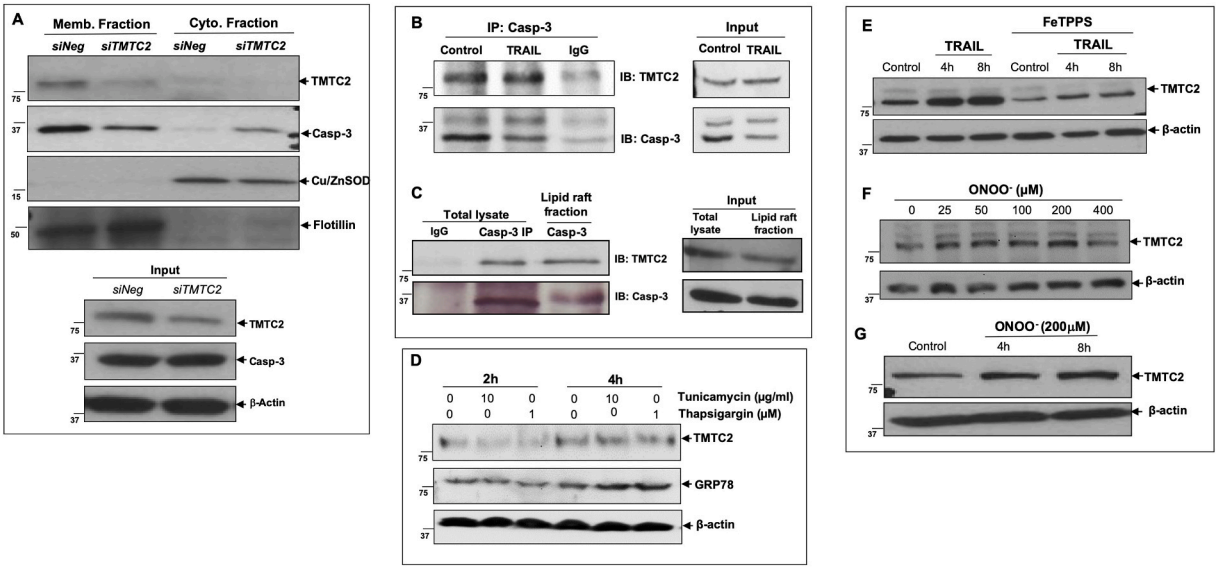

Fig. 6. TMTC2 co-precipitates with caspase-3 and its TRAIL-induced induction is $ONOO^-$ dependent (A) TMTC2 is detected in the membrane fraction and its gene knockdown reduces caspase-3 membrane localization. HK-1 cells were transfected with *siTMTC2* (50 nM) for 48 h and membrane or cytosolic fractions were obtained by centrifugation as described in Materials and Methods. Proteins from the individual fractions were subjected to Western blot analysis using anti-TMTC2 and anti-caspase-3. Flotillin was used as a membrane-specific probe while Cu/Zn SOD expression was used as a cytosol-specific control. (B) Whole cell lysates from HK-1 cells treated with TRAIL (25 ng/ml for 6 h) were immunoprecipitated with anti-caspase-3 and probed using anti-TMTC2 or anti-caspase-3 by Western blotting (C) Whole cell lysate and lipid raft fraction from HK-1 cells were immunoprecipitated with anti-caspase-3 and probed with anti-TMTC2 or anti-caspase 3 by Western blotting. (D) ER stress does not induce TMTC2. HK-1 cells were treated with tunicamycin (10 μg/ml) or thapsigargin (1 μM) for 2 h or 4 h and whole cell lysates were probed for the expression of TMTC2 and GRP78 by Western blotting. (E) HK-1 cells were pre-treated with FeTPPS (50 μM for 1 h) followed by 2 h or 4 h incubation with 25 ng/ml of TRAIL and protein levels of TMTC2 were determined by Western blotting (F) HK-1 cells were exposed to increasing concentrations of $ONOO^-$ (25 μM–400 μM) for 6 h or (G) 200 μM for 4hrs or 8 h and TMTC2 expression was probed in whole cell lysates using Western blotting.

specifically involves intracellular increase in $ONOO^-$.

2.5. TRAIL responsiveness of NPC cells is TMTC2 dependent

Next, we looked at the involvement of TMTC2 in the sensitivity of NPC cells to TRAIL-induced apoptosis. To do so, the expression of TMTC2 was manipulated in the two cell lines by either siRNA mediated gene silencing in HK-1 cells or overexpression in C666-1 cells. Transfection (48 h) with *siTMTC2* resulted in a significant decrease (20% vs 43% in *siNeg* transfected cells) in sub-G1 fraction in response to TRAIL (24 h), suggestive of lowered DNA fragmentation (Fig. 7A). Conversely, overexpression of TMTC2 (48 h) in C666-1 cells resulted in a significant increase (30% vs 20% in EV transfected cells) in sub-G1 fraction upon incubation with TRAIL (Fig. 7B). Supporting these results, knockdown of *TMTC2* in HK-1 cells significantly inhibited caspase processing while its upregulation in C666-1 resulted in a marked increase in the cleaved (processed/active) forms of caspase-8, -9 and -3 (Fig. 7C). These data were corroborated by changes in overall cell survival (Supplementary Figure S4A&B). Furthermore, as activation of NF-κB activation has been linked to TRAIL-induced signaling through TRAIL-R1 (DR4), TRAIL-R2 (DR5) and TRAIL-R4 [34], we also questioned the role of NF-κB in TRAIL-induced TMTC2 upregulation and apoptosis. Interestingly, pharmacological inhibition of NF-κB signaling (JSH-23; 25 μM), evidenced by the decrease in IκB phosphorylation, repressed TRAIL-induced induction of TMTC2 (Fig. 7D), thus suggesting regulation of TMTC2 by NF-κB. It is to be noted that in contrast to JSH-23, another pharmacological inhibitor of NF-κB not only amplified TRAIL induced processing of caspase-3 and cleavage of PARP, but further enhanced TRAIL induced induction of TMTC2 (Supplementary Figure S3D). However, celastrol is a quinone methide triterpene that can target multiple signaling pathways by ROS generation as well as modulate members of JNK, Akt/mTOR, NF-κB, STAT3/JAK2, HSP90, Cdc37, p23, Erα, etc [35] Therefore, it becomes imperative that the role of NF-κB be evaluated using more direct approaches such as using a knock-out of p65. Taken together, these data provide a hitherto novel mechanism involving the upregulation of TMTC2 as a critical factor in the responsiveness of NPC cells to TRAIL-mediated apoptosis, which could have potential implications for expanding our understanding on the role of this transmembrane protein in death receptor ligation and downstream signaling, in particular changes in cellular redox milieu.

2.6. TRAIL is a potential NPC therapeutic

To ascertain the potential of TRAIL as a therapy against NPC, we performed bioinformatics analysis on cBioPortal. We first selected the GDAC Firehose Legacy Head and Neck squamous cell carcinoma study (as this database has mRNA expression) and queried for correlation between the expression of *TMTC2* and TRAIL receptors *DR4/5* as well as between *TMTC2* and *caspases*. A highly significant, though mildly positive, correlation was observed between *TMTC2* and *DR4* as well as *TMTC2* and *caspase-3* (Fig. 8A). Likewise, the correlation between *TMTC2* and *DR5* expression was highly significant, albeit weakly positive (Fig. 8A). Since TMTC2 protein expression was integral to caspase-3 membrane localization as well as initiation of the apoptotis pathway, we next questioned the association between *TMTC2* expression and patient survival in the same GDAC Firehose Legacy Head and Neck squamous cell carcinoma study on cBioPortal. An arbitrary OQL was submitted to define high *TMTC2* and low *TMTC2* expression levels to be: *TMTC2*: Exp >1 as $TMTC2^{high}$ and *TMTC2*: Exp < -1 as $TMTC2^{low}$ groups, respectively. Serendipitously, our findings suggested that patients with $TMTC2^{low}$ had a significantly poorer 5-year overall as well as disease-free survival (Fig. 8B). The median patient survival in both analyses also indicated that the period of survival was reduced in half in patients with $TMTC2^{low}$, compared to those with $TMTC2^{high}$, thus affirming that

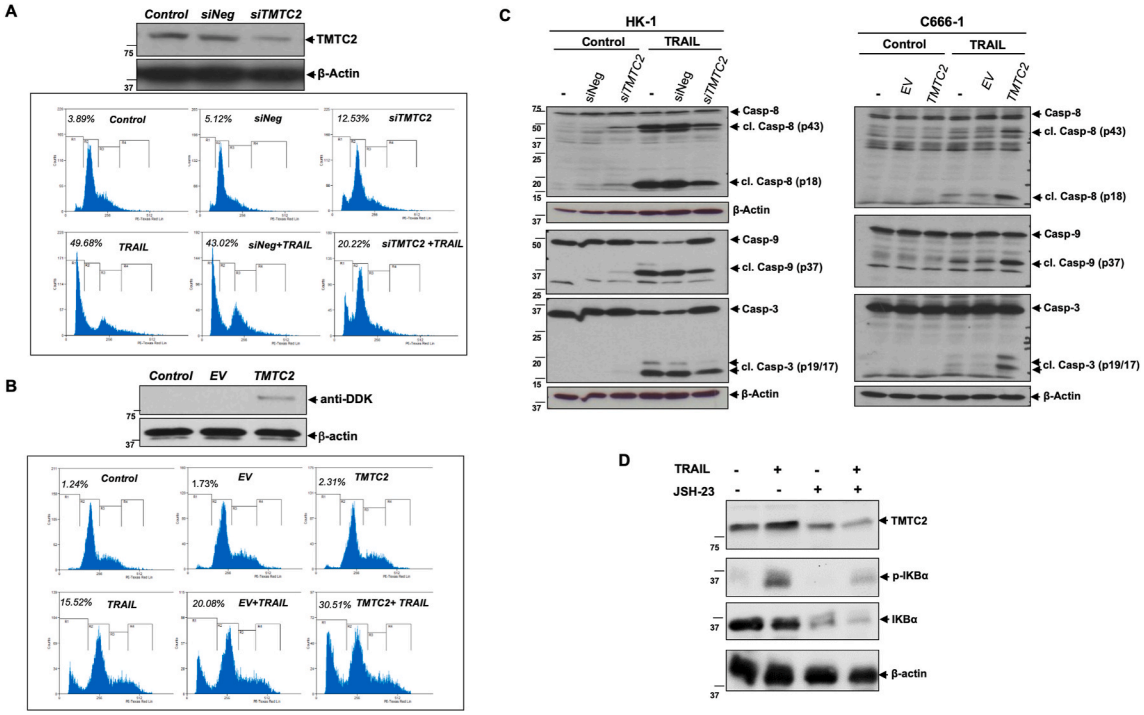

Fig. 7. TRAIL-induced apoptosis in NPC cells is TMTC2 dependent (A) HK-1 cells were transfected with *siTMTC* (50 nM) or *siNeg* for 48 h followed by exposure to 25 ng/ml of TRAIL for 24 h and cell cycle analysis for sub-G1 population (%) was performed using PI as described in Materials and Methods. (B) C666-1 cells were transfected with vector containing *TMTC2* (4 μg for 48 h) as described in Materials and Methods. Transiently transfected cells were exposed to 100 ng/ml of TRAIL and cell cycle analysis for sub-G1 population (%) was performed using PI as described in Materials and Methods. (C) *TMTC2* knock-down with *siTMTC2* in HK-1 cells prevents cleavage of caspases −8,-9 and −3 by TRAIL (25 ng/ml for 6 h) and conversely, *TMTC2* overexpression in C666-1 cells enhanced the processing of the respective caspases. (D) HK-1 cells were treated with 25 ng/ml of TRAIL with or without 18 h pre-incubation with JSH-23 (25 μM) and cell lysates were probed for TMTC2, pIκBα, and IKBα using Western blotting.

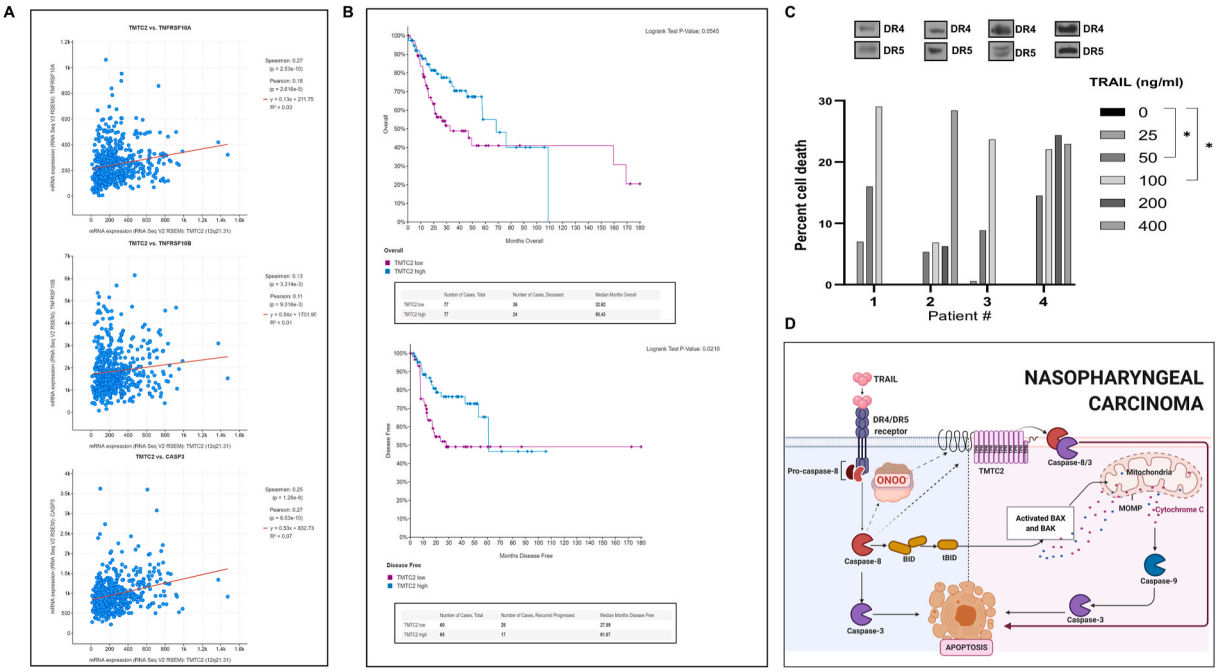

Fig. 8. TRAIL is a potential adjuvant therapeutic in NPC (A) 530 samples from TCGA, GDAC Firehose Legacy Head and Neck squamous cell carcinoma on cBioPortal were queried for correlation between TRAIL receptors *DR4 (TNFRSF10A)* or *DR5 (TNFRSF10B)* and *TMTC2* mRNA as well as between *TMTC2* and *caspase-3* mRNA. Highly significant and mildly positive correlation was detected for all three comparisons in this dataset. (B) Samples from TCGA, GDAC Firehose Legacy Head and Neck squamous cell carcinoma on cBioPortal were queried for correlation of *TMTC2* mRNA with overall survival or disease-free survival, respectively. Specifically, low *TMTC2* expression correlated with significantly poorer disease-free median survival. (C) Primary cells derived from NPC patients were treated *ex vivo* with TRAIL (25–400 ng/ml for 48 h) and cell viability was determined by the MTT assay as described in materials and Methods. Two-way ANOVA was employed for statistical analysis and all comparisons were normalized to untreated control ($* = p < 0.05$). Protein expression of DR4 and DR5 in patient-derived biopsies was assessed by Western blot. (D) Schematic model of TRAIL-induced apoptosis in NPC cells. Ligation of the death receptors induces caspase-8 dependent upregulation of TMTC2, which further amplifies death signaling via membrane co-localization with caspase-3. TMTC2 upregulation is downstream of TRAIL-induced increase in intracellular $ONOO^-$.

higher *TMTC2* correlated with better disease prognosis. To validate these data *in vivo*, we acquired primary cells from biopsies of NPC patients and subjected them to incremental doses of TRAIL (0–400 ng/ml). Notably, DR4 and DR5 were detected in the whole cell lysates of primary NPC cells obtained from 4 patients, all of which exhibited significant sensitivity to TRAIL (Fig. 8C). It is also worth pointing out that the sensitivity of HK-1 and C666-1 cell lines to TRAIL was comparable to that of conventional chemotherapy drugs, 5 Fluorouracil (5FU) and cisplatin (Supplementary Figure S5), thus supporting the potential for targeting death receptors as a management strategy against NPC.

Finally, we pooled 5 different studies on cBioPortal [(Head and Neck Squamous Cell Carcinoma (Broad, Science 2011), Head and Neck Squamous Cell Carcinoma (Johns Hopkins, Science 2011), Head and Neck Squamous Cell Carcinoma (TCGA, Firehose Legacy), Nasopharyngeal Carcinoma (Singapore, Nat Genet 2014), Oral Squamous Cell Carcinoma (MD Anderson, Cancer Discov 2013)] to query for mutations in *DR4 or DR5* or *TMTC2* in head and neck cancers. Firstly, the frequency of mutations in these genes appears to be extremely low, and secondly not only are the consequences of these mutations poorly defined, but also the analysis indicates that all mutations in the receptors were deep deletions (Supplementary Figure S6A). To validate the clinical nature of these mutations, we also queried if these mutations presented with better or poorer prognosis, when compared to the non-mutated group. Our results, albeit in a very few samples (n = 2 with mutations each in *DR4/DR5* receptors and n = 12 with mutations in *TMTC2*), indicated poorer prognosis in patients harbouring the mutations (Supplementary Figure S6B). These data seem to suggest that, while mutations in these genes might be rare, once mutated they could be associated with poorer prognosis. As such, in the majority of NPC patients, activation of death receptor signaling and/or screening for agents that induce TMTC2 upregulation could be attractive adjuvant approaches against NPC.

3. Discussion

We present evidence that NPC cell lines and primary cells derived from patient biopsies exhibit detectable levels of functional death receptors, DR4 and DR5, which upon ligation with TRAIL undergo caspase-8 driven Type II apoptosis. Interestingly, events downstream of death receptor ligation include alteration in cellular redox status, specifically an increase in $ONOO^-$, early activation and recruitment of caspase-3 in the membrane fractions, and most importantly, upregulation of a hitherto less well-studied membrane protein, TMTC2, which co-precipitated with caspase-3 in the lipid raft fractions. Bioinformatics analyses also indicate remarkably low mutation rates for either *DR4/DR5* or *TMTC2* in NPC patients, and notably poorer survival in $TMTC2^{low}$ patients.

NPC, a non-lymphomatous, squamaous cell carcinoma is endemic in Southern China, parts of Southeast Asia and Mediterranean Basin, and its management includes radiotherapy, chemotherapy and occasionally surgery. Radiotherapy is brought with the potential of severely damaging the sensitive areas around the tumor, while the two drugs of choice, 5-FU and cisplatin, elicit off-target toxicity and select for drug resistance clones with the risk of disease relapse. As such, identification of novel modalities to target NPC are highly desirable, as their use as adjuvants with conventional approaches could allow for the reduction of therapeutic doses, thereby alleviating untoward side effects. Given the observations that DR4 and/or DR5 are selectively expressed by tumor cells, results indicating death receptors on the cell surface of NPC cells and their responsiveness to TRAIL could be worthy of exploring as a potential treatment strategy. As a matter of fact, Phase I clinical studies

have established the safety and tolerability of recombinant human TRAIL (rhTRAIL) or the agonistic monoclonal anti-DR4 or anti-DR5 antibody in human cancer. Moreover, Phase II trials are currently evaluating the therapeutic efficacy of TRAIL agonists as single agents or in combination with established cancer therapeutics. While the cascade of events observed upon death receptor ligation are classical and rather well established, albeit not extensively reported for NPC cells, there are three novel and interesting findings unraveled in this study.

3.1. Membrane localization of caspase-3 in NPC cells

Firstly, the presence of pro-caspase-3 in the membrane fractions of NPC cell lines, as shown by its presence in the lipid raft fractions colocalized with caveolin-1, and its early enzymatic activation upon exposure to TRAIL. Canonically, caspase proteases have been described as cytosolic, however, there are several instances where membrane recruitment has been documented. In terms of the latter, most of the studies report nuclear recruitment of initiator or executioner caspases, despite the fact that only caspase-2 possesses a nuclear localization sequence [36]. Caspase-3 being the predominant executioner caspase during apoptosis triggered by diverse stimuli, including death receptor ligation, its membrane localization and early activation suggests a possible proximity to the DISC assembly in the lipid raft domains, as was demonstrated by previous reports [37,38]. Similarly, membrane lipid raft localization of caspase-3 has been reported in Jurkat leukemia cells and peripheral T lymphocytes [32]. Also, spontaneous activation of membrane bound pro-caspase-3, regulated by Bcl-2, was demonstrated in human lymphobastoid cells [39], which is rather intriguing considering the absence of a membrane localizing sequence. Our present findings corroborate the constitutive presence of pro-caspase-3, unlike other reports where stimulus-induced recruitment was reported [40], in the membrane fractions of NPC cells.

3.2. TMTC2: a novel mediator of death receptor signaling in NPC cells

Secondly, our investigations revealed the involvement of a multipass transmembrane protein, TMTC2, in the membrane localization of pro-caspase-3 in NPC cells. TMTC2 is an ER-resident protein that was identified mainly in regulating Ca^{2+} homeostasis by its interaction with the SERCA2B pump and calnexin; overexpression results in lower ER Ca^{2+} uptake thus disturbing cytosloic-ER Ca^{2+} traffic [23]. TMT2 (and TMTC1) has also been proposed to reside in large multi-protein complexes, and shown to be a mannosyltransferase, wherein it transfers mannosyl residues to hydroxyl groups of serine and threonine residues [41]. Our results provide evidence for protein-protein interaction between TMTC2 and pro-caspase-3 in the lipid raft fractions. Interestingly, knockdown of *TMTC2* significantly reduced membrane localization of pro-caspase-3, thus suggesting a role in membrane tethering of caspase-3. It is highly unlikely that TMTC2 is a caspase-3 substrate, as no proteolytic cleavage is observed upon the activation of caspase-3. Moreover, TMTC2 knockdown seems to block TRAIL-induced caspase-3 processing, thus indicating that TMTC2 is an upstream mediator of TRAIL-induced apoptotic execution. We also report that TMTC2 is constitutively expressed in a host of human cancer cell lines, however, it remains to be seen whether its involvement in membrane recruitment of caspase-3 is limited to NPC cells. Interestingly, the level of expression of TMTC2 in the two cell lines correlates with the sensitivity to TRAIL-induced apoptosis; HK-1 cells express higher levels of TMTC2 and are significantly more sensitive to TRAIL than C666-1 cells. Remarkably too, the expression of TMTC2 is significantly induced in a time dependent manner upon ligation of the death receptors, and modulating the expression of TMTC2 impacts TRAIL sensitivity of NPC cells; *TMTC2* knockdown inhibits TRAIL-induced apoptosis in HK-1 cells while its overexpression in C666-1 cells enhances their TRAIL responsiveness. Notably, despite the fact that structurally and functionally TMTC1-4 proteins have been proposed as ER-resident proteins, stimuli that induce ER stress, such as tunicamycin and thapsigragin, did not affect the cellular levels of TMTC2, thereby indicating that the involvement in cell fate signaling might be a novel function of this family, or at least TMTC2. Whether TMTC1, 3 or 4 elicits similar effect(s) remains to be elucidated. Although, in the present study TMTC2 appears to play a role as a mediator of TRAIL-induced apoptosis, the possibility that TMTC2 impacts receptor clustering in the lipid raft domains could not be ruled out. To that end, adhesion proteins, such as cadherins [42], could possibly play a role in the functional biology of TMTC2 from the standpoint of receptor-mediated apoptosis or/and caspase-3 localization. It is also worth mentioning that O-linked glycosylation of death receptors have been shown to trigger ligand-stimulated clustering of DR4 and DR5 [43]. Whether TMTC2 has a role to play in that would be worth exploring. Finally, considering the association of EBV infection in the biology of NPC, the involvement of viral proteins such as latent membrane protein1 (LMP1) in the induction and/or membrane recruitment of pro-caspase-3 can also not be ruled out. In this regard, not only caspase-3 was shown to proteolytically cleave LMP1, but more importantly, LMP1 expression was reported to induce the expression of caspase-3 [44].

3.3. Peroxynitrite mediates TRAIL-induced induction of TMTC2 and apoptosis

Thirdly, TRAIL-induced induction of TMTC2 and downstream caspase activation are mediated by intracellular $ONOO^-$, a product of the reaction between $O_2^{\cdot-}$ and nitric oxide (NO), and a critical second messenger involved in various physiological and/or pathological processes [45]. Interestingly, an early increase in TRAIL-mediated $ONOO^-$ is caspase-8 dependent, which further amplifies downstream signaling. Scavening $ONOO^-$ not only blocked TRAIL-induced apoptosis, but also inhibited the increase of TMTC2 expression, thereby providing evidence that TRAIL-induced upregulation of TMTC2 is redox mediated. The intermediary role of $ONOO^-$ is further corroborated by results indicating the lack of an effect of other ROS species, such as $O_2^{\cdot-}$ and H_2O_2.

The dichotomy of the different ROS/RNS and their cellular concentrations on cancer cell survival and apoptosis sensitivity has been demonstrated by our group using a variety of model systems, including death receptor signaling [19–22,46–49]. These studies demonstrate that a moderate increase in $ONOO^-$ blocks death receptor signaling while higher levels trigger apoptotic execution. Also, earlier studies have provided evidence to link $ONOO^-$ to the direct or indirect activation of caspases, in particular caspase-3 [50–52]. Here we show that TRAIL induced increase in $ONOO^-$ is downstream of caspase-8 activation and its degradation (by FeTPPS) blocks TMTC2 upregulation, thus unraveling a probable mechanism linking death receptor ligation-mediated increase in RNS to NPC cell death. As TMTC2 induction appears to be at the mRNA level, it is likely that $ONOO^-$ positively impacts the promoter region of *TMTC2* with predicted binding sites for a number of transcription factors including Myc, NF-κB, HIF, MyoD and Max1 [53]. Canonically, TNF-R ligation results in apoptosis/necrosis as well as NF-κB activation, which promotes cell survival. Interestingly, we obtained conflicting results using two different inhibitors of NF-κB activity, celastrol [54] and JSH-23 [55]; celestrol further increased TMTC2 while JSH-23 significantly blocked its induction upon TRAIL treatment. Since JSH-23 is a more specific inhibitor of NF-κB activity (nuclear localization) the significant inhibition of TMTC2 suggests involvement of NF-κB in TRAIL-induced TMTC2 induction, which validates our recent findings linking intracellular peroxynitrite to NF-κB activation [49]. The opposing effect of celestrol could very well be due to the myriad signaling nodes (other than NF-κB) regulated by this natural compound such as JNK, Akt/mTOR, STAT3/JAK2, HSP90, Cdc37, p23, ERα, etc. [54] These results suggest the possibility of $ONOO^-$ dependent involvement of NF-κB in TRAIL-induced induction of TMTC2, however, the molecular mechanisms of how this is accomplished is worthy of further investigated.

3.4. Clinical relevance of TMTC2 and DR4/5 expression in NPC

The therapeutic potential of targeting death receptor activation as a possible novel strategy against NPC is supported by the expression level as well as responsiveness of patient-derived primary cells. Despite the relatively small sample size, the fact that tumor cells express functional death receptors provides a proof-of-concept for the use of TRAIL as an adjuvant therapy in the overall management of NPC. This is further corroborated by bioinformatics data indicating significant correlation between mRNA expression of *TMTC2* and *TNFRSF10A(DR4)/ TNFRSF10B (DR5)* as well as *TMTC2* and *caspase-3*. The correlation is much stronger between *TMTC2* and *DR4*, compared to *DR5*, which is also supported by the data from NPC cell lines indicating DR4 as being the predominant functional death receptor. Earlier reports have also demonstrated DR4 as the main effector in the increased TRAIL sensitivity of melanoma cells [56] as well as lung, colon and breast cancer cells [57–60]. Notably, the 5-year disease-free survival is significantly better in patients with $TMTC2^{high}$ than those in the $TMTC2^{low}$ category, which suggests that *TMTC2* levels could be used as a predictor of disease progression/prognosis as well as for stratifying NPC patients for potential TRAIL therapy. Furthermore, bioinformatics data suggesting the relatively low incidence of mutations in *DR4/DR5*, and more importantly the association between the mutations (3%) and poorer survival argue in favor of considering death receptor ligation (recombinant TRAIL or anti-DR4/DR5 antibodies) as a treatment option for NPC.

4. Materials and Methods

4.1. Cell culture

Human NPC cell lines, HK-1 and C666-1, were generously provided by Dr. Hsieh Wen-Son (CSI, NUS) and maintained in RPMI 1640 (Hyclone Logan, Utah, USA) supplemented with 1% L-glutamine, 1% streptomycin-penicillin and 10% FBS. All cell lines were grown and passaged in a humidified incubator at 37 °C with 5% CO_2. Cells were routinely screened for mycoplasma and all experiments were performed exclusively with mycoplasma-negative cells.

4.2. Reagents and chemicals

TRAIL was purchased from Biomol (Plymouth Meeting, PA, USA). Propidium iodide (PI), Crystal violet, Bromophenol blue, DMSO, Tween 20, EDTA, DTT, Sucrose, HEPES, Tris and Glycine were purchased from Sigma Aldrich (St. Louis, MO, USA). Pan-caspase inhibitor ZVAD-fmk was obtained from Alexis Biochemicals, Lausen, Switzerland. Transfection reagents, Superfect and Dharmafect, were procured from Qiagen (Hilden, Germany) and Thermo Scientific (Waltham, MA, USA), respectively. CM-H2DCFDA and fluorogenic substrates of caspase-8, -9 and -3 were purchased from Invitrogen (Eugene, Oregon, USA). FeTPPS (*5,10,15,20-tatrakis(4-sulfonatophenyl)porphyrinato iron (III) chloride*) was purchased from Merck (Darmstadt, Germany) and $ONOO^-$ was obtained from Cayman Chemical (Ann Arbor, MI, USA). Coomassie Blue protein concentration reagent was obtained from Pierce Biotechnology (Rockford, IL, USA). 10X phosphate buffered saline (PBS), 10X SDS, Tris-HCl buffer (pH 7.4) were purchased from NUMI Media Preparation Facility (National University of Singapore).

4.3. Antibodies

The following antibodies were used in the study.

Antibody	Catalog #	Company	Application
Cytochrome-C	12963	Cell Signaling Technologies	Western Blotting
Bid	8762	Cell Signaling Technologies	Western Blotting
Cu/Zn SOD	4266	Cell Signaling Technologies	Western Blotting
Caspase-3	9668	Cell Signaling Technologies	Western Blotting
Caspase-3	sc-7272	Santa Cruz Biotechnologies	Western Blotting/IP
Caspase-8	9746	Cell Signaling Technologies	Western Blotting
Caspase-8	sc-56070	Santa Cruz Biotechnologies	Western Blotting/IP
Caspase-9	9502	Cell Signaling Technologies	Western Blotting
VDAC	sc-390996	Santa Cruz Biotechnologies	Western Blotting
Bcl-2	sc-7382	Santa Cruz Biotechnologies	Western Blotting
β-Actin	sc-47778	Santa Cruz Biotechnologies	Western Blotting
GAPDH	sc-25778	Santa Cruz Biotechnologies	Western Blotting
DR4	sc- 8411	Santa Cruz Biotechnologies	Western Blotting
DR4	sc- 6824	Santa Cruz Biotechnologies	Western Blotting
DR4	FAB347P	R&D Systems	Flow Cytometry/ Confocal analysis
DR5	sc- 7192	Santa Cruz Biotechnologies	Western Blotting
DR5	sc- 65314	Santa Cruz Biotechnologies	Western Blotting
DR5	FAB6311P	R&D Systems	Flow Cytometry/ Confocal analysis
DDK	TA50011-100	Origene	Western Blotting
Mn SOD	611580	BD Biosciences	Western Blotting
TMTC2	ARP49065_P050	Aviva System Biology	Western Blotting
TMTC2	AV49064	Sigma-Aldrich	Western Blotting
Caveolin-1	ab2910	Abcam	Western Blotting
Flotillin	ab13493	Abcam	Western Blotting

Secondary antibodies for western blotting were obtained from Pierce Chemical Co. (Rockford, IL, USA), while secondary antibodies for flow cytometry/confocal analyses were obtained from Invitrogen, (Eugene, Oregon, USA).

4.4. cDNA synthesis and QPCR

Samples were harvested in TRIZOL purchased from Ambion, Invitrogen (Carlsbad, CA, USA). RNA extraction was performed using the phenol-chloroform-isopropanol extraction method. The following primer sequences for *TMTC2* were used for cDNA synthesis: *Forward (5′-3′) GACTGCGATCAGGAATGGAGAC and Reverse (5′-3′) TGACTCTTCA-GAACATTTCCAAGG*. cDNA synthesis was performed according to the manufacturer's instructions using the Onescript Plus™ cDNA Synthesis Kit from Applied Biological Materials (Vancouver, Canada). The final cDNA product was stored at −20 °C for subsequent experiments. QPCR was performed using SYBR Select from Thermo Scientific (Waltham, MA, USA). Quantitation of mRNA was performed on a 384-well format white bottom plate on the LightCycler 480 Instrument-II, Roche Life-Science (Basel, Switzerland).

4.5. DNA and siRNA transfections

pcDNA3-Bcl-2 was a generous gift from Dr. Elizabeth Yang (Vanderbilt University, USA). *pcDNA3.1* empty vector was obtained from Invitrogen (Carlsbad, CA, USA). *pCMV6* empty vector and *pCMV6-Myc-DDK-TMTC2* plasmids were obtained from Origene (Rockville, MD, USA). siRNAs for *DR4* and *DR5* as well as the scrambled siRNA were obtained from Dharmacon Technologies, Thermo Scientific, (Waltham,

MA). siRNAs for *caspase-3* and *caspase-8* were obtained from Qiagen (Hilden, Germany). siRNAs for *TMTC2* was obtained from Invitrogen (Carlsbad, CA, USA). For transient overexpression of Bcl-2, HK-1 cells were seeded at 0.3×10^6 cells/well in a 6-well tissue culture plate. 48 hrs later, cells were transfected with 2 μg of *pcDNA3-Bcl-2* or *pcDNA3.1 (vector alone)* using Superfect transfection reagent according to manufacturer's instructions. Cells were cultured for 24 h after transfection before performing subsequent treatments. For transient overexpression of TMTC2, HK-1 or C666-1 cells were seeded at 0.4×10^6 cells/well and 0.8×10^6 cells/well, respectively, in a 6-well tissue culture plate 24 h prior to transfection, followed by 4 μg of *pCMV6-Myc-DDK-TMTC2* or *pCMV6* using Superfect transfection reagent according to standard protocol provided by the manufacturer. Cells were subsequently cultured for 48 h prior to subsequent treatments. To knock-down *DR4* and *DR5*, *siDR4 (*100 nM) or *siDR5* (50 nM) or equivalent concentrations of scrambled *siRNA* were transfected into cells using the Dharmafect 1 transfection reagent according to standard instructions provided by the manufacturer. Cells were subsequently cultured for 24 h for *DR5* knock-down and 48 h for *DR4* knock-down before further treatments. To knock-down *caspase-3*, *caspase-8*, and *TMTC2*, 50 nM of respective *siRNAs* or scrambled *siRNA* were transfected into cells using Dharmafect 1 transfection reagent according to the standard protocol provided by the supplier and allowed to recover for up to 48 h post-transfection.

4.6. Cell viability determination

Crystal violet assay: HK-1 (0.1×10^5 cells/well) and C666-1 (0.2×10^5 cells/well) cells were seeded in a 24-well plate, 48 h prior to treatment. Subsequently, cells were exposed to different concentrations of TRAIL (25 ng/ml to 100 ng/ml) for 24 h. Next, cells were washed once with 1X PBS before addition of 0.2 ml of Crystal violet solution (0.75% crystal violet in 50% ethanol:distilled water with 1.75% formaldehyde and 0.25% NaCl and stored at RT) to each well and incubation for 10 min. The excess crystal violet was washed off with distilled water. The non-viable cells gets detached and washed off in the process leaving the attached viable cells that retain crystal violet. Crystals were dissolved in 1% SDS (in 1X PBS) and viability was determined by reading absorbance at wavelength 595 nm using a TECAN spectrophotometer (Mannedorf, Switzerland).

MTT assay: To assess cell viability in NPC primary cells, tissue biopsies was obtained upon informed consent from NPC patients at National University Hospital, Singapore (DSRB 200500264). Single cell suspension was obtained from the biopsy material and 5000 cells/well were seeded into a 96-well tissue culture plate and incubated with TRAIL (50–200 μg/ml) for 48 h. Next, MTT solution (3–5 mg/ml in PBS) was added to each well and the plate was incubated at 37 °C for 2 h. The plate was then centrifuged at 4000 rpm for 20 min at RT and supernatant was aspirated. Crystals were dissolved in DMSO and viability was determined by reading absorbance at wavelength 570 nm using a TECAN spectrophotometer.

4.7. Determination of tumor colony forming ability

HK-1 (0.1×10^5 cells/well) and C666-1 (0.2×10^5 cells/well) cells were plated in a 24-well plate 48 h prior to treatment with TRAIL (25 ng/ml to 100 ng/ml) for 8 h. Following a wash, 10,000 cells from each sample were re-plated into 100 mm culture plates. Plates were then incubated for 10–14 days to allow for colony formation and stained with crystal violet for qualitative assessment of the colony forming ability.

4.8. Propidium iodide (PI) staining for DNA fragmentation analysis

Following experimental treatments, the cells were washed and resuspended in 1 ml of 1X PBS and immediately fixed with 70% ethanol while vortexing. Samples were subsequently incubated for 30 min at 4 °C before washing twice with 1X PBS. Samples were finally resuspended in 500 μl PI:RNase A solution for 2 h at 37 °C for DNA content analysis. PI:RNAse A solution was prepared as: 1/50 volume of PI stock (*50X PI stock solution was dissolved in* 38 mM *sodium citrate buffer to a stock concentration of 0.*5 mg/ml *and stored in the dark at* 4^oC) and 1/40 volume of RNAse A stock (*RNAse A was dissolved in* 10 mM *Tris-HCl (*pH *7.5) and* 15 mM *NaCl to a stock concentration of* 10 mg/ml *and kept at* -20^0C) were mixed in 38 mM citrate buffer. At least 10,000 events were analyzed by flow cytometry (Beckman Coulter, USA) with the excitation set at 488 nm and emission at 610 nm.

4.9. Measurement of caspase enzymatic activities

Caspases −8, −9 and −3 activities were assayed using AFC-conjugated substrates. HK-1 (0.4×10^6 cells/well) and C666-1 (0.8×10^6 cells/well) cells were plated 48 h prior to treatment; TRAIL 25 ng/ml for HK-1 and 100 ng/ml for C-6661 for 2 h, 4 h, 8 h, 16 h and 24 h. Cells were then harvested and washed with 1X PBS and resuspended in chilled cell lysis buffer from BD Pharmingen (San Diego, CA, USA). Samples were incubated on ice for 30 min prior to incubation with AFC conjugated substrates and real-time measurements of enzyme-catalyzed release of AFC were obtained with a TECAN spectrophotometer. The absorbances were normalized against the protein concentration of samples and plotted as x-fold increase in caspase activity over the untreated control cells.

4.10. Measurement of mitochondrial transmembrane potential

To measure mitochondrial transmembrane potential ($\Delta\Psi_m$), cells (1×10^6) were treated with TRAIL (12.5 ng/ml or 50 ng/ml for HK-1 cells; 50 ng/ml or 100 ng/ml for C666-1 cells) for 2 h. Cells were loaded with 40 nM DiOC6 (3,3′-dihexyloxacarbocyanine Iodide) and following a 30 min incubation analyzed by flow cytometry. The uncoupler CCCP (Carbonyl cyanide 3-chlorophenyhydrazone), obtained from Sigma-Aldrich (St Louis, MO, USA), was used as a positive control to induce depolarization and added to cells 30 min prior to harvesting. At least 10,000 events were analyzed by WinMD1 software. Data shown are representative of at least 3 independent experiments.

4.11. Western blot analysis

Whole cell protein extracts were harvested in RIPA lysis buffer (50 mM *Tris-HCl* pH *7.5,* 150 mM *NaCl, 1% v/v deoxycholic acid, 0.1% v/v SDS and* 1 mM *EDTA).* Before use, the buffer was supplemented with protease inhibitors *(*1 mM *PMSF,* 10 μg/ml *aprotinin,* 20 μg/ml *pepstatin A)* and phosphatase inhibitors *(*1 mM *NaF,* 1 mM Na_3VO_4) with 1% NP-40. Protein concentration was quantified using the Coomassie blue reagent. Equal amounts of proteins from the lysates were mixed with 5X Laemmli loading dye (*3.*1 ml *of* 100 mM *Tris-HCL* pH *6.8, 1 g SDS (10%),* 2 ml *glycerol (20%), 2.*5 ml *β-mercaptoethanol (25%), 0.01 g bromophenol blue (0.1%), top to* 10 ml *with 2.*4 ml *distilled* H_2O). and boiled for 10 min. The samples were then subjected to SDS-PAGE and subsequently transferred to PVDF membranes. The membranes were blocked with 5% (w/v) fat-free milk in TBST (*2 L TBS (*500 ml *of 1 M Tris-HCl (*pH *7.4) with 87.6 g of NaCl in 10 L of distilled water) with* 2 ml *of Tween-20 and stored at RT*) for 1 h and washed thrice with TBST to remove excess milk. Subsequently, the membranes were probed with the relevant primary antibodies overnight at 4 °C on a rocker. The membrane was washed thrice to remove unbound primary antibody and probed again using appropriate HRP-conjugated secondary antibody in TBST containing 5% (w/v) fat-free milk at room temperature for 1 h. After three washes with TBST to remove any excess unbound secondary antibody, the proteins of interest were detected with ECL chemiluminescence detection substrates using Kodak Biomax MR X-ray film in the dark room or by using the ChemiDoc (Thermo Scientific, Waltham, MA, USA).

4.12. Isolation of cytosolic, mitochondria and plasma membrane fractions

Cells were harvested, washed once with cold 1X PBS and subsequently transferred to extraction buffer and incubated on ice for 10 min. Cells were then homogenized (10 strokes for HK-1 cells and 20 strokes for C666-1 cells) before centrifugation at 1000*g* for 10 min at 4 °C. Next, the supernatant was centrifuged at 10,000 *g* for 20 min at 4 °C. The pellet obtained, the mitochondria fraction, was dissolved in RIPA lysis buffer. The supernatant was centrifuged at 100,000 *g* for 1 h at 4 °C. The pellet, plasma membrane fraction, was isolated into RIPA lysis buffer. The supernatant containing the cytosolic fraction was also stored.

4.13. Isolation of membrane lipid rafts by sucrose gradient ultracentrifugation

HK-1 and C666-1 cells (2×10^6 cells and 4×10^6 cells, respectively) were seeded in 10 cm petri dishes 48 h prior to treatment. After respective treatments were performed, cells were harvested and washed with ice-cold 1X PBS before incubating in 500 ml of HEPES buffer (25 mM *HEPES,* 150 mM *NaCl,* pH*7.4 containing* 1 mM *PMSF,* 10 mg/ml *aprotinin,* 20 mg/ml *pepstatin A and* 10 mg/ml *leupeptin*) containing 1% TritonX-100 for 10 min on ice. Lysates were then subjected to 1 round of freeze thaw before homogenizing (20 strokes) with a Dounce 60 homogenizer. Subsequently, the lysates were centrifuged at 400 *g* for 10 min at 4 °C. Next, the supernatant was transferred to a new tube and passed through a 27 G syringe for further lysis. Samples were then sonicated (3 sets of 10 s pulses at 40 V). Protein concentration using the Coomassie assay, as mentioned before, was performed and 1 mg of protein was mixed with HEPES buffer to obtain an overall volume of 0.5 ml for each sample and the samples transferred to an ultracentrifuge tube. Next, an equal volume of 80% sucrose (w/v) in HEPES buffer was carefully added to the tube and mixed with the lysate. Following this, 2 ml of 30% sucrose (w/v) and 2 ml of 5% sucrose (w/v) in HEPES buffer were further added to the tube carefully from the top. The sucrose gradient was then subjected to centrifugation for 21 h at 4 °C in a Beckman ultracentrifuge at 32,000 rpm. Post centrifugation, the samples were divided into nine 0.5 ml fractions. 40 μl was taken from each fraction and subjected to western blotting.

4.14. Analysis of cell surface levels of DR4 and DR5

HK-1 and C666-1 cells were plated in a 12 well plate at densities of 0.3×10^6 cells/well and 0.6×10^6 cells/well, respectively, for 48 h prior to treatment and/or analysis. After relevant treatments, cells were harvested and subjected to 3 washes with 1X PBS supplemented with 0.5% FBS. Next, cells were incubated with phycoerythrin (PE)-conjugated mouse monoclonal anti-human DR5 or DR4 for 45 min at 4 °C. Cells were subsequently washed and resuspended in 1X PBS for further analysis by flow cytometry (excitation wavelength of 488 nm). The PE-conjugated mouse IgG2B was used as an isotype control. Data was analyzed using WinMDI software.

4.15. Confocal microscopy

UV treated sterile polylysine coverslips were first placed into 12 well plates and culture media was added. HK-1 and C666-1 cells (1×10^5 and 2×10^5, respectively) were then seeded into the plate and 48 h later subjected to the various treatments. Next, cells were washed twice with ice cold 1X PBS and fixed with 2% paraformaldehyde. Cells were then washed with PBS thrice and subsequently permeabilized with 0.1% Triton-X at room temperature for 10 min. Cells were again washed thrice with ice cold 1X PBS before blocking them for 1 h with 5% BSA (in 1X PBS). Subsequently, cells were incubated with either mouse anti-caspase-3 (1:200) or mouse anti-DDK (for detection of overexpressed TMTC2 at 1:200) and rabbit anti-caveolin (1:400) in 1X PBS with 5% BSA for 2 h at RT. Next, the wells were washed thrice with 5% BSA (ice cold) followed by incubation for an hour in 1:300 dilution for Alexafluor-488 anti-mouse secondary antibody (Invitrogen) and 1:400 dilution for Alexafluor-568 anti-rabbit secondary antibody (Invitrogen) in 1X PBS with 5% BSA. Cells were finally washed three times with ice cold 1X PBS before the coverslips were mounted with DAPI on glass slides. Samples were imaged with Olympus Fluoview FV1000 confocal microscope and images were analyzed using Olympus Fluoview 1.7 viewer.

4.16. Co-immunoprecipitation (Co-IP) assay

Post treatment, cells were washed with ice cold 1X PBS followed by incubation in Co-IP buffer (50 mM *Tris-HCl,* 150 mM *NaCl,* pH*7.4 containing 0.5% NP-40,* 1 mM *PMSF,* 10 mg/ml *aprotinin,* 20 mg/ml *pepstatin A,* 10 mg/ml *leupeptin*) at 4 °C for 30 min with constant agitation. Subsequently, lysates were centrifuged at 12,000 rpm for 10 min. The pellet was discarded, and the supernatant was incubated with protein A or G agarose beads for 1 h on a rotator with constant agitation. Subsequently, the samples were centrifuged at 12,000 rpm for 10 min at 4 °C. The supernatant was transferred to a fresh tube and 1 mg of the supernatant was subsequently incubated with 4 μg of the relevant primary antibody or control IgG of the same species overnight on a rotator at 4 °C. The next day protein A or G agarose beads were added to each of the samples and rotated for another 4 h at 4 °C. The complexes were then washed thrice with the Co-IP buffer, centrifuged at 12,000 rpm for 5min at 4 °C before boiling for 30 min in 1X Laemmli loading buffer. Samples were subsequently analyzed by western blotting.

4.17. Detection of intracellular ROS/RNS

CM-H2DCFDA (5- (and-6)- chloromethyl- 2′,7′- dichlorodihydrofluorescein diacetate, acetyl ester) staining was used to detect intracellular ROS. Cells (1×10^6/ml) were washed once with 1X PBS and resuspended in 1X PBS containing 10 μM CM-H2DCFDA and incubated at 37 °C in the dark for 20 min. Next, cells were centrifuged at 1500 rpm for 5 min and resuspended in 1X PBS. Samples were then analyzed by flow cytometry. At least 10,000 events were analyzed (excitation: 488 nm and emission: 525 nm) using the WinMDI software. Final fluorescence values obtained were normalized against the untreated control and plotted as x-fold increase in fluorescence over the untreated control.

4.18. cBioPortal data analyses

The cBioPortal platform [61,62] was used to query five different Head and Neck cancer studies [63–67] for mutations, copy number alterations and mRNA expression analysis of genes in this study.

4.19. Statistical analyses

All experiments subjected to statistical analyses were repeated for a minimum of 3 times. Numerical data are presented as mean ± SD. Comparisons were normalized to control unless otherwise specified. ANOVA analyses (using GraphPad Prism, GSL Biotech LLC, CA, USA) were performed in cases were three or more comparisons were required. For other cases, paired student's t-test (two-tail, unequal variance) was employed. Statistical significance was set at $p < 0.05$.

Declaration

Several images included in this manuscript have been adapted from the PhD thesis (National University of Singapore) of the second author Patricia Tay.

Declaration of competing interest

All authors concur with the decision to submit this original work to *Redox Biology* and none of the authors have any conflict of interest to declare.

Acknowledgements

The authors would like to thank Dr. Thomas Loh (ENT, National University Hospital, Singapore) for providing the clinical samples. Patricia Tay is currently at Singapore Clinical Research Institute, Singapore. Dan Liu is currently at Siemens Diagnostics, Singapore. This work was supported by grant from the Singapore Cancer Syndicate (SCS-NPU0094R) to SP.

Appendix A. Supplementary data

Supplementary data to this article can be found online at https://doi.org/10.1016/j.redox.2021.102193.

References

[1] Y.-P. Chen, et al., Nasopharyngeal carcinoma, Lancet 394 (10192) (2019) 64–80.
[2] F. Bray, et al., Global cancer statistics 2018: GLOBOCAN estimates of incidence and mortality worldwide for 36 cancers in 185 countries, Ca - Cancer J. Clin. 68 (6) (2018) 394–424.
[3] L.S. Young, C.W. Dawson, Epstein-Barr virus and nasopharyngeal carcinoma, Chin. J. Cancer 33 (12) (2014) 581–590.
[4] M.K. Kam, et al., Prospective randomized study of intensity-modulated radiotherapy on salivary gland function in early-stage nasopharyngeal carcinoma patients, J. Clin. Oncol. 25 (31) (2007) 4873–4879.
[5] Y.P. Mao, et al., Prognostic factors and failure patterns in non-metastatic nasopharyngeal carcinoma after intensity-modulated radiotherapy, Chin. J. Cancer 35 (1) (2016) 103.
[6] B. Zhang, et al., Intensity-modulated radiation therapy versus 2D-RT or 3D-CRT for the treatment of nasopharyngeal carcinoma: a systematic review and meta-analysis, Oral Oncol. 51 (11) (2015) 1041–1046.
[7] K.H. Park, et al., Concurrent chemoradiation followed by adjuvant chemotherapy in patients with locoregionally advanced nasopharyngeal carcinoma in Korea, Cancer Chemother. Pharmacol. 66 (4) (2010) 643–651.
[8] A.W. Lee, et al., Randomized trial of radiotherapy plus concurrent-adjuvant chemotherapy vs radiotherapy alone for regionally advanced nasopharyngeal carcinoma, J. Natl. Cancer Inst. 102 (15) (2010) 1188–1198.
[9] P. Blanchard, et al., Chemotherapy and radiotherapy in nasopharyngeal carcinoma: an update of the MAC-NPC meta-analysis, Lancet Oncol. 16 (6) (2015) 645–655.
[10] A.W. Lee, et al., Factors contributing to the efficacy of concurrent-adjuvant chemotherapy for locoregionally advanced nasopharyngeal carcinoma: combined analyses of NPC-9901 and NPC-9902 Trials, Eur. J. Cancer 47 (5) (2011) 656–666.
[11] Y.M. Tian, et al., Prognostic model for survival of local recurrent nasopharyngeal carcinoma with intensity-modulated radiotherapy, Br. J. Cancer 110 (2) (2014) 297–303.
[12] W.-L. Tan, et al., Advances in systemic treatment for nasopharyngeal carcinoma, Chin. Clin. Oncol. 5 (No 2) (April 2016). Chinese Clinical Oncology (Nasopharyngeal Carcinoma-Guest Editors: Joseph Wee, Yoke-Lim Soong, Melvin Chua), 2016.
[13] Y. Zhan, S. Fan, Multiple mechanisms involving in radioresistance of nasopharyngeal carcinoma, J. Cancer 11 (14) (2020) 4193–4204.
[14] E. Gallmeier, et al., Loss of TRAIL-receptors is a recurrent feature in pancreatic cancer and determines the prognosis of patients with no nodal metastasis after surgery, PLoS One (2) (2013) 8, e56760-e56760.
[15] L. Kriegl, et al., Expression, cellular distribution, and prognostic relevance of TRAIL receptors in hepatocellular carcinoma, Clin. Cancer Res. 16 (22) (2010) 5529–5538.
[16] Y. Kojima, et al., Importin β1 protein-mediated nuclear localization of death receptor 5 (DR5) limits DR5/tumor necrosis factor (TNF)-related apoptosis-inducing ligand (TRAIL)-induced cell death of human tumor cells, J. Biol. Chem. 286 (50) (2011) 43383–43393.
[17] R.M. Pitti, et al., Induction of apoptosis by Apo-2 ligand, a new member of the tumor necrosis factor cytokine family, J. Biol. Chem. 271 (22) (1996) 12687–12690.
[18] S. Wang, W.S. El-Deiry, TRAIL and apoptosis induction by TNF-family death receptors, Oncogene 22 (53) (2003) 8628–8633.
[19] M.V. Clement, J.L. Hirpara, S. Pervaiz, Decrease in intracellular superoxide sensitizes Bcl-2-overexpressing tumor cells to receptor and drug-induced apoptosis independent of the mitochondria, Cell Death Differ. 10 (11) (2003) 1273–1285.
[20] T.W. Poh, et al., LY303511 amplifies TRAIL-induced apoptosis in tumor cells by enhancing DR5 oligomerization, DISC assembly, and mitochondrial permeabilization, Cell Death Differ. 14 (10) (2007) 1813–1825.
[21] S. Seah, et al., Activation of surrogate death receptor signaling triggers peroxynitrite-dependent execution of cisplatin-resistant cancer cells, Cell Death Dis. 6 (10) (2015) e1926-e1926.
[22] J.L. Hirpara, et al., Superoxide induced inhibition of death receptor signaling is mediated via induced expression of apoptosis inhibitory protein cFLIP, Redox Biol. 30 (2020) 101403.
[23] J.C. Sunryd, et al., TMTC1 and TMTC2 are novel endoplasmic reticulum tetratricopeptide repeat-containing adapter proteins involved in calcium homeostasis, J. Biol. Chem. 289 (23) (2014) 16085–16099.
[24] M. MacFarlane, et al., TRAIL receptor-selective mutants Signal to Apoptosis via TRAIL-R1 in primary lymphoid malignancies, Cancer Res. 65 (24) (2005) 11265.
[25] C.R. Reis, et al., Rapid and efficient cancer cell killing mediated by high-affinity death receptor homotrimerizing TRAIL variants, Cell Death Dis. 1 (10) (2010) e83-e83.
[26] V. Tur, et al., DR4-selective tumor necrosis factor-related apoptosis-inducing ligand (TRAIL) variants obtained by structure-based design, J. Biol. Chem. 283 (29) (2008) 20560–20568.
[27] E. Bremer, et al., Targeted delivery of a designed sTRAIL mutant results in superior apoptotic activity towards EGFR-positive tumor cells, J. Mol. Med. (Berl.) 86 (8) (2008) 909–924.
[28] E.W. Duiker, et al., Enhanced antitumor efficacy of a DR5-specific TRAIL variant over recombinant human TRAIL in a bioluminescent ovarian cancer xenograft model, Clin. Cancer Res. 15 (6) (2009) 2048.
[29] H. Lee, et al., DR4-Ser424 O-GlcNAcylation promotes Sensitization of TRAIL-tolerant Persisters and TRAIL-resistant cancer Cells to death, Cancer Res. 79 (11) (2019) 2839.
[30] J. Hirpara, et al., Metabolic reprogramming of oncogene-addicted cancer cells to OXPHOS as a mechanism of drug resistance, Redox Biol. 25 (2019) 101076.
[31] K. Iskandar, et al., Synthetic lethality of a novel small molecule against mutant KRAS-expressing cancer cells involves AKT-dependent ROS production, Antioxidants Redox Signal. 24 (14) (2016) 781–794.
[32] S.M. Aouad, et al., Caspase-3 Is a Component of fas death-inducing signaling Complex in lipid Rafts and its activity is Required for complete caspase-8 Activation during fas-mediated cell death, J. Immunol. 172 (4) (2004) 2316.
[33] J. Beaudouin, et al., Caspase-8 cleaves its substrates from the plasma membrane upon CD95-induced apoptosis, Cell Death Differ. 20 (4) (2013) 599–610.
[34] M.A. Degli-Esposti, et al., The novel receptor TRAIL-R4 induces NF-kappaB and protects against TRAIL-mediated apoptosis, yet retains an incomplete death domain, Immunity 7 (6) (1997) 813–820.
[35] J. Shi, et al., Celastrol: a Review of useful strategies Overcoming its Limitation in anticancer application, Front. Pharmacol. 11 (2020) 1726.
[36] P.A. Colussi, N.L. Harvey, S. Kumar, Prodomain-dependent nuclear localization of the caspase-2 (Nedd2) precursor. A novel function for a caspase prodomain, J. Biol. Chem. 273 (38) (1998) 24535–24542.
[37] B. Oxhorn, I. Buxton, Caveolar compartmentation of caspase-3 in cardiac endothelial cells, Cell. Signal. 15 (2003) 489–496.
[38] M.A. Secinaro, et al., Glycolysis promotes caspase-3 activation in lipid rafts in T cells, Cell Death Dis. 9 (2) (2018) 62.
[39] J.F. Krebs, et al., Activation of membrane-associated procaspase-3 is regulated by Bcl-2, J. Cell Biol. 144 (5) (1999) 915–926.
[40] E.A. Prokhorova, et al., Apoptosis regulation by subcellular relocation of caspases, Sci. Rep. 8 (1) (2018) 12199.
[41] I.S.B. Larsen, et al., Multiple distinct O-Mannosylation pathways in eukaryotes, Curr. Opin. Struct. Biol. 56 (2019) 171–178.
[42] I.S.B. Larsen, et al., Discovery of an O-mannosylation pathway selectively serving cadherins and protocadherins, Proc. Natl. Acad. Sci. U. S. A. 114 (42) (2017) 11163–11168.
[43] K.W. Wagner, et al., Death-receptor O-glycosylation controls tumor-cell sensitivity to the proapoptotic ligand Apo2L/TRAIL, Nat. Med. 13 (9) (2007) 1070–1077.
[44] S. Togi, et al., Caspase-dependent cleavage regulates protein levels of Epstein-Barr virus-derived latent membrane protein 1, FEBS Lett. 590 (6) (2016) 808–818.
[45] R. Radi, Oxygen radicals, nitric oxide, and peroxynitrite: Redox pathways in molecular medicine, Proc. Natl. Acad. Sci. U. S. A. 115 (23) (2018) 5839–5848.
[46] S. Pervaiz, et al., Activation of the RacGTPase inhibits apoptosis in human tumor cells, Oncogene 20 (43) (2001) 6263–6268.
[47] K.A. Ahmad, et al., Hydrogen peroxide-mediated cytosolic acidification is a signal for mitochondrial translocation of Bax during drug-induced apoptosis of tumor cells, Cancer Res. 64 (21) (2004) 7867–7878.
[48] D. Raman, et al., Peroxynitrite promotes serine-62 phosphorylation-dependent stabilization of the oncoprotein c-Myc, Redox Biol. 34 (2020) 101587.
[49] Y.H. Yee, et al., Sustained IKKβ phosphorylation and NF-κB activation by superoxide-induced peroxynitrite-mediated nitrotyrosine modification of B56γ3 and PP2A inactivation, Redox Biol. 41 (2021) 101834.
[50] S. Zhuang, G. Simon, Peroxynitrite-induced apoptosis involves activation of multiple caspases in HL-60 cells, Am. J. Physiol. Cell Physiol. 279 (2) (2000) C341–C351.
[51] K. Dohi, et al., Peroxynitrite and caspase-3 expression after ischemia/reperfusion in mouse cardiac arrest model, in: Brain Edema XII, Springer Vienna, Vienna, 2003.
[52] J.J. Shacka, et al., Two distinct signaling pathways regulate peroxynitrite-induced apoptosis in PC12 cells, Cell Death Differ. 13 (9) (2006) 1506–1514.
[53] S. Fishilevich, et al., GeneHancer: genome-wide integration of enhancers and target genes in GeneCards, Database (2017) 2017.
[54] J. Shi, et al., Celastrol: a Review of useful strategies Overcoming its Limitation in anticancer application, Front. Pharmacol. 11 (2020) 558741.

[55] H.M. Shin, et al., Inhibitory action of novel aromatic diamine compound on lipopolysaccharide-induced nuclear translocation of NF-kappaB without affecting IkappaB degradation, FEBS Lett. 571 (1–3) (2004) 50–54.
[56] B.M. Kurbanov, et al., Efficient TRAIL-R1/DR4-mediated Apoptosis in melanoma Cells by tumor necrosis factor-related apoptosis-inducing ligand (TRAIL), J. Invest. Dermatol. 125 (5) (2005) 1010–1019.
[57] K. Kim, et al., Molecular determinants of response to TRAIL in killing of normal and cancer cells, Clin. Cancer Res. 6 (2) (2000) 335.
[58] J. Sträter, et al., Expression of TRAIL and TRAIL receptors in colon carcinoma: TRAIL-R1 is an independent prognostic parameter, Clin. Cancer Res. 8 (12) (2002) 3734–3740.
[59] I. Kazhdan, R.A. Marciniak, Death receptor 4 (DR4) efficiently kills breast cancer cells irrespective of their sensitivity to tumor necrosis factor-related apoptosis-inducing ligand (TRAIL), Cancer Gene Ther. 11 (10) (2004) 691–698.
[60] Z. Jin, et al., Deficient tumor necrosis factor-related apoptosis-inducing ligand (TRAIL) death receptor transport to the cell surface in human colon cancer cells selected for resistance to TRAIL-induced apoptosis, J. Biol. Chem. 279 (34) (2004) 35829–35839.
[61] E. Cerami, et al., The cBio cancer genomics portal: an open Platform for exploring multidimensional cancer genomics data, Cancer Discov. 2 (5) (2012) 401.
[62] J. Gao, et al., Integrative analysis of complex cancer genomics and clinical profiles using the cBioPortal, Sci. Signal. 6 (269) (2013) pl1.
[63] N. Stransky, et al., The mutational landscape of head and neck squamous cell carcinoma, Science 333 (6046) (2011) 1157–1160.
[64] N. Agrawal, et al., Exome sequencing of head and neck squamous cell carcinoma reveals inactivating mutations in NOTCH1, Science 333 (6046) (2011) 1154–1157.
[65] M.S. Lawrence, et al., Comprehensive genomic characterization of head and neck squamous cell carcinomas, Nature 517 (7536) (2015) 576–582.
[66] C.R. Pickering, et al., Integrative genomic characterization of oral squamous cell carcinoma identifies frequent somatic drivers, Cancer Discov. 3 (7) (2013) 770–781.
[67] D.C. Lin, et al., The genomic landscape of nasopharyngeal carcinoma, Nat. Genet. 46 (8) (2014) 866–871.